Naval Research Laboratory
Stennis Space Center, MS 39529-5004

NRL/FR/7174--93-9420

Volume Reverberation in the Fram Strait Marginal Ice Zone: May 1988

MARCIA A. WILSON

Ocean Acoustics Branch
Center for Environmental Acoustics

August 3, 1993

Approved for public release; distribution unlimited.

REPORT DOCUMENTATION PAGE

Form Approved
OBM No. 0704-0188

1. AGENCY USE ONLY *(Leave blank)*	2. REPORT DATE	3. REPORT TYPE AND DATES COVERED
	August 3, 1993	Final

4. TITLE AND SUBTITLE

Volume Reverberation in the Fram Strait Marginal Ice Zone: May 1988

5. FUNDING NUMBERS

Job Order No. 5715254A3
Program Element No. 0602435N
Project No. RJ35I21
Task No.
Accession No. DN496443

6. AUTHOR(S)

Marcia A. Wilson

7. PERFORMING ORGANIZATION NAME(S) AND ADDRESS(ES)

Naval Research Laboratory
Center for Environmental Acoustics
Stennis Space Center, MS 39529-5004

8. PERFORMING ORGANIZATION REPORT NUMBER

NRL/FR/7174--93-9420

9. SPONSORING/MONITORING AGENCY NAME(S) AND ADDRESS(ES)

Naval Research Laboratory
Center for Environmental Acoustics
Stennis Space Center, MS 39529-5004

10. SPONSORING/MONITORING AGENCY REPORT NUMBER

11. SUPPLEMENTARY NOTES

12a. DISTRIBUTION/AVAILABILITY STATEMENT

Approved for public release; distribution unlimited

12b. DISTRIBUTION CODE

13. ABSTRACT *(Maximum 200 words)*

At frequencies between 3 and 50 kHz, high volume reverberation levels can have a limiting effect on active sonar operations. Therefore, experiments were conducted by the Naval Research Laboratory to determine the reverberation levels in the marginal ice zone. Three volume reverberation data sets were collected in May 1988 between Greenland and Spitsbergen in the Fram Strait. Data include frequencies from 3.5 to 50 kHz for downward-looking transducers and 3.5 to 12 kHz for an upward-looking configuration. Pulses of 10 and 40 ms in duration were used. Returning signals were processed to show depths and intensities of volume scattering. Layer strengths and column strengths are shown as a function of frequency. Column strengths are compared to those from the Chukchi Sea marginal ice zone and from locations near Greenland and Iceland.

14. SUBJECT TERMS	15. NUMBER OF PAGES
Acoustics, Arctic, Physical Oceanography	32
	16. PRICE CODE

17. SECURITY CLASSIFICATION OF REPORT	18. SECURITY CLASSIFICATION OF THIS PAGE	19. SECURITY CLASSIFICATION OF ABSTRACT	20. LIMITATION OF ABSTRACT
Unclassified	Unclassified	Unclassified	Same as report

CONTENTS

BACKGROUND AND MEASUREMENTS 1

ENVIRONMENT IN FRAM STRAIT 4

Physical Oceanography 4
Fram Strait Pelagic Food Chain 5

DATA ANALYSIS 7

RESULTS 10

Scattering Strength vs. Depth 10
Layer and Column Strengths 23

DISCUSSION 25

CONCLUSIONS 28

ACKNOWLEDGMENTS 28

REFERENCES 29

VOLUME REVERBERATION IN THE FRAM STRAIT MARGINAL ICE ZONE: MAY 1988

BACKGROUND AND MEASUREMENTS

On 2 May 1988, a party of 14 scientists from the Naval Research Laboratory (NRL), the Applied Physics Laboratory, University of Washington (APL/UW), the Arctic Submarine Laboratory (ASL), Ocean Sensors, Inc., and Planning Systems, Inc. (PSI) sailed from Reykjavik, Iceland, with the crew of the USCGC *Northwind* to the Fram Strait area indicated in Fig. 1. Extensive environmental measurements were made in support of this exercise in the marginal ice zone (MIZ 88) [1]. The USCGC *Northwind* sailed to the west of Iceland and northeast along the ice edge to about 79°N, then went into the ice, found a suitable ice floe, and moored to the floe while an ice camp was established. Although various acoustic experiments were done at this ice camp, the volume reverberation experiment will be the only focus of this report.

With help from the U.S. Coast Guard, everything needed to live and work on the ice was offloaded to the floe on 9–10 May. Camp consisted of a bunk tent, a mess tent, an electronics tent, and an environmental tent. A 1-m^2 hole was drilled through about 4 m of ice near the electronics tent for placing the high-frequency volume reverberation equipment in the water. The ice camp was located about 1000 m from the southern edge of a nearly circular floe with a diameter of about 3 mi.

During the volume reverberation measurements, the floe drifted gradually from Station 1 at 79°11′ N, 0°19′ E on 15 May; to 78°55′ N, 1°43′ W on Station 2, 17 May; to 78°48′ N, 2°29′ W at Station 3 on 18 May. The lower, expanded part of Fig. 1 shows water depths between 2000 and 3000 m beneath the ice camp, which floated westward from Station 1 to Station 3 [1].

To decrease interference with the experiments from ship noise, the *Northwind* moved to a location about 8 mi northeast of camp on the morning of 15 May while the volume reverberation equipment was tested. Five calibrated EDO Western transducers generated and received high-frequency acoustic pulses. Model 311 was used for 50 kHz; model 6303 for 40 and 45 kHz; model 6232 for 25 and 30 kHz; model 6230 for 16 and 20 kHz; and model 515 for 3.5, 5.0, 7.5, and 12.0 kHz. A sequence of 10 or more pulses, 9.6 s apart, was transmitted for each frequency. A pulse length of 10 ms was used at frequencies from 3.5 to 30 kHz. A 40-ms pulse was transmitted for frequencies from 16 to 50 kHz.

Volume reverberation in the lower water column was measured with the transducers suspended 4 to 5 m below the ice and pointing down. To measure reverberation in the upper 30 m, the transducers were placed, facing up, 65 m below the surface for frequencies from 3.5 to 12 kHz.

Figure 2 is a block diagram of hardware used in the field. The volume reverberation system allowed the operator to vary the frequency, pulse length, pulse interval, and gains. It was used

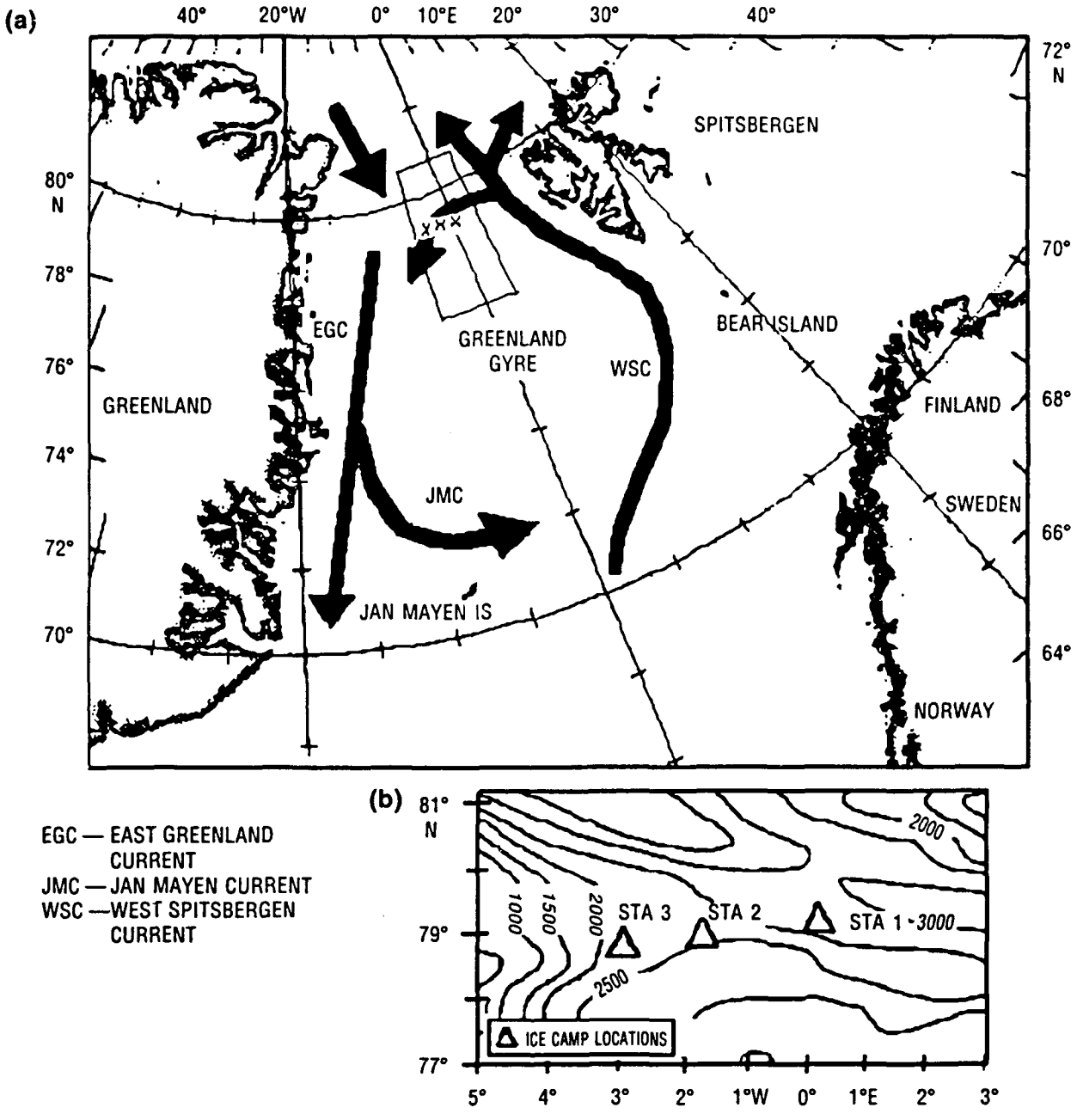

Fig. 1 — (a) Locations of volume reverberation measurement sites, marked "x," and major currents of the surrounding area and (b) expanded area and local bathymetry.

to control and monitor the output, to switch the transducer between transmit and receive modes, to amplify and filter the input signal, to take the envelope of the received signal, and to record the results. Volume reverberation data were stored on two FM channels of a Racal Store 7 tape recorder with the output current and a time code on other channels. Recording began at least a few seconds before the first ping in a sequence and continued until well after the last ping in that sequence.

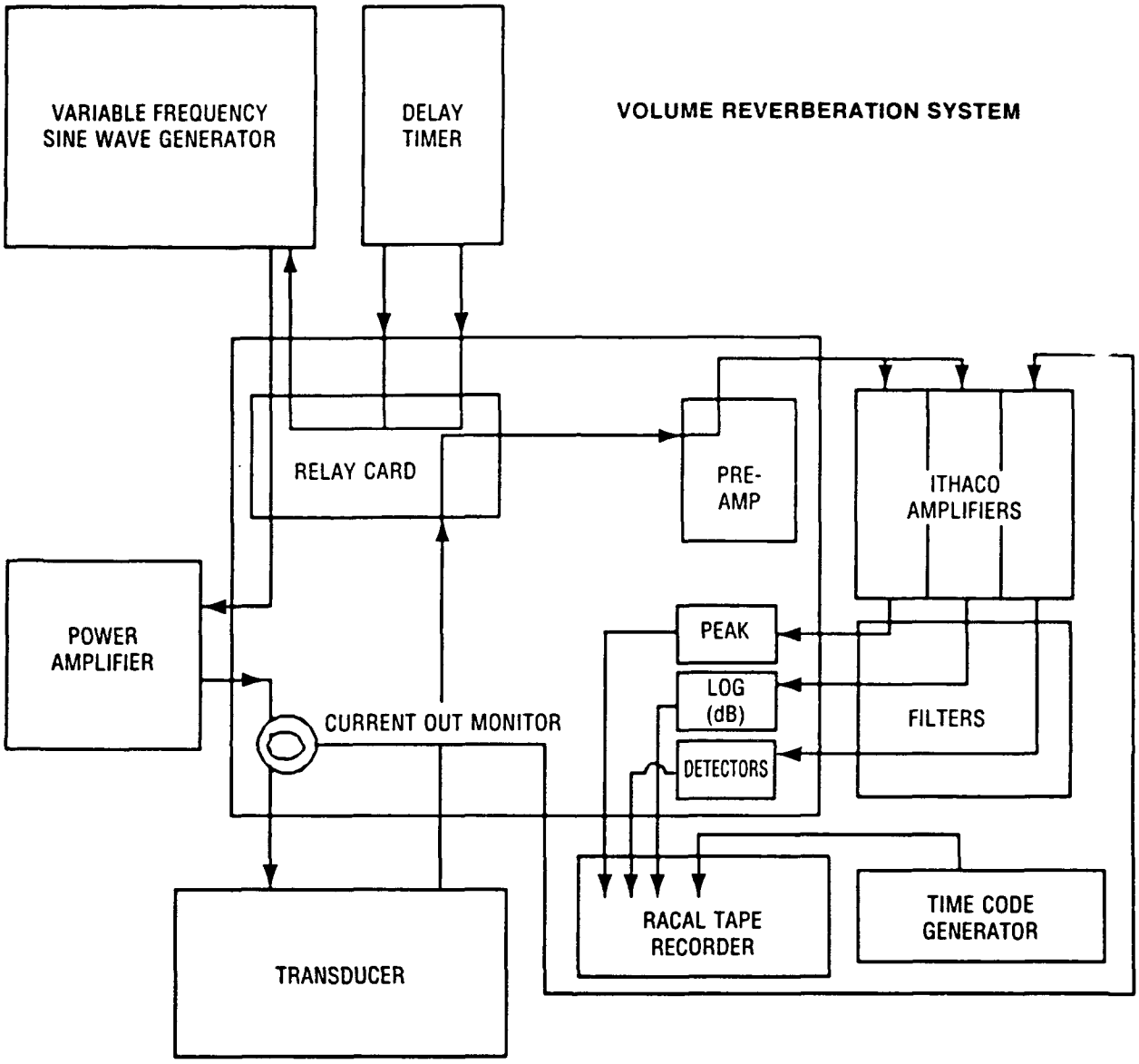

Fig. 2 — Basic hardware used in MIZ 88 volume reverberation experiment.

Running the power amplifier output through the volume reverberation system induced large signals in the return circuits which overloaded amplifiers when they were properly set for recording the returning signal. Thus, after the direct signal, the higher gain channel shows a large negative rebound that obscures part of the reverberation. Gains for two data channels, filter settings, amperes to the transducer, input volts, pulse length, frequency, and time were recorded on the log sheets for each set of data taken. A calibration run was also recorded during the experiment.

Data collection began for Station 1 at 1513 local time on 15 May, and continued until 2225, when the sun was low along the horizon. Only downward-looking data were taken on Station 1. Downward- and upward-looking measurements were made at Station 2 between 1609 and 2105 on

17 May. On 18 May, large noise levels prevented the collection of data with the 515 transducer at Station 3; therefore, 16 kHz was the lowest frequency in that set. Data were collected from 1438 to 1700. Only downward-looking data were taken at Station 3.

The last of the other experiments was completed by midnight, 20 May. The scientists and equipment boarded the *Northwind* about 1700 on 21 May and returned to Reykjavik.

ENVIRONMENT IN FRAM STRAIT

Physical Oceanography

The location of the ice edge in Fram Strait is fairly consistent throughout the year because new ice is continually advected from the Arctic Ocean [2]. Fram Strait is in the northern portion of the Greenland Gyre, which is a counterclockwise circulation bounded by Greenland to the west, Jan Mayen to the south, and Spitsbergen to the northeast (Fig. 1). The West Spitsbergen Current brings water from the North Atlantic northward into the Arctic Ocean and branches to the west near Spitsbergen about 79°N. The East Greenland Current carries polar water south along the eastern coast of Greenland. The Jan Mayen Current branches off from the East Greenland Current north of Jan Mayen and turns to the east. The southward-flowing East Greenland Current dominates the circulation in the upper 500 m of the 1988 exercise area. The current is composed mostly of Atlantic Intermediate Water (AIW); acoustic sound velocities are greater than 1445 m/s.

The AIW, found at depths between 50 and 300 m, is brought across the Fram Strait by the West Spitsbergen Current and is mixed with polar water. Above the AIW in the surface layer is the polar water in which sound speeds are less than 1445 m/s. Between the cold polar water and the warmer AIW is a thermocline at which water temperature increases from less than −1°C to between +1° and +2°C.

In the upper layer the salinity is around 34 ppt, but below 130 m it increases to about 34.6 ppt. On 15–18 May, salinity, temperature, and sound speed changes occurred rapidly—from 70 to 130 m, as shown in Fig. 3. The thermoclines at Stations 1 and 2 begin about 20 m deeper and are noticeably steeper than that at Station 3 [1]. The MIZ 88 experiment site is in the same area as the Polar Front, where water temperature is 0°C at 100-m depth.

The Fram Strait is about 450 km wide between Greenland and Spitsbergen. The MIZ 88 ice camp was within 50 km of the 5600 m water of the Molloy Deep, the deepest part of the Arctic Ocean [3], where a nearly permanent gyre brings increased mixing and nutrients into the upper portion of the water column [4]. Other passages between the Arctic Ocean and subarctic waters are much shallower.

High windspeeds made the below-freezing air temperatures seem even colder. In addition to making working conditions more difficult, high winds increase the noise, including high-frequency transients, by adding to the rate of movement of the ice in the water. The windspeed at 1500 just before data collection began on 15 May was below 13 kt, but by 1700 it was up to 17 kt and stayed that high. Gusts were up to 27 kt until after data collection was completed that day. At Station 1 there was a 4-h break between 7.5- and 16-kHz data. Although the sun never set completely, the difference in solar energy received before and after the break was significant. The surface temperature decreased from −2.7°C to −6.2°C during that time. Winds continued to be high at Station 2, where

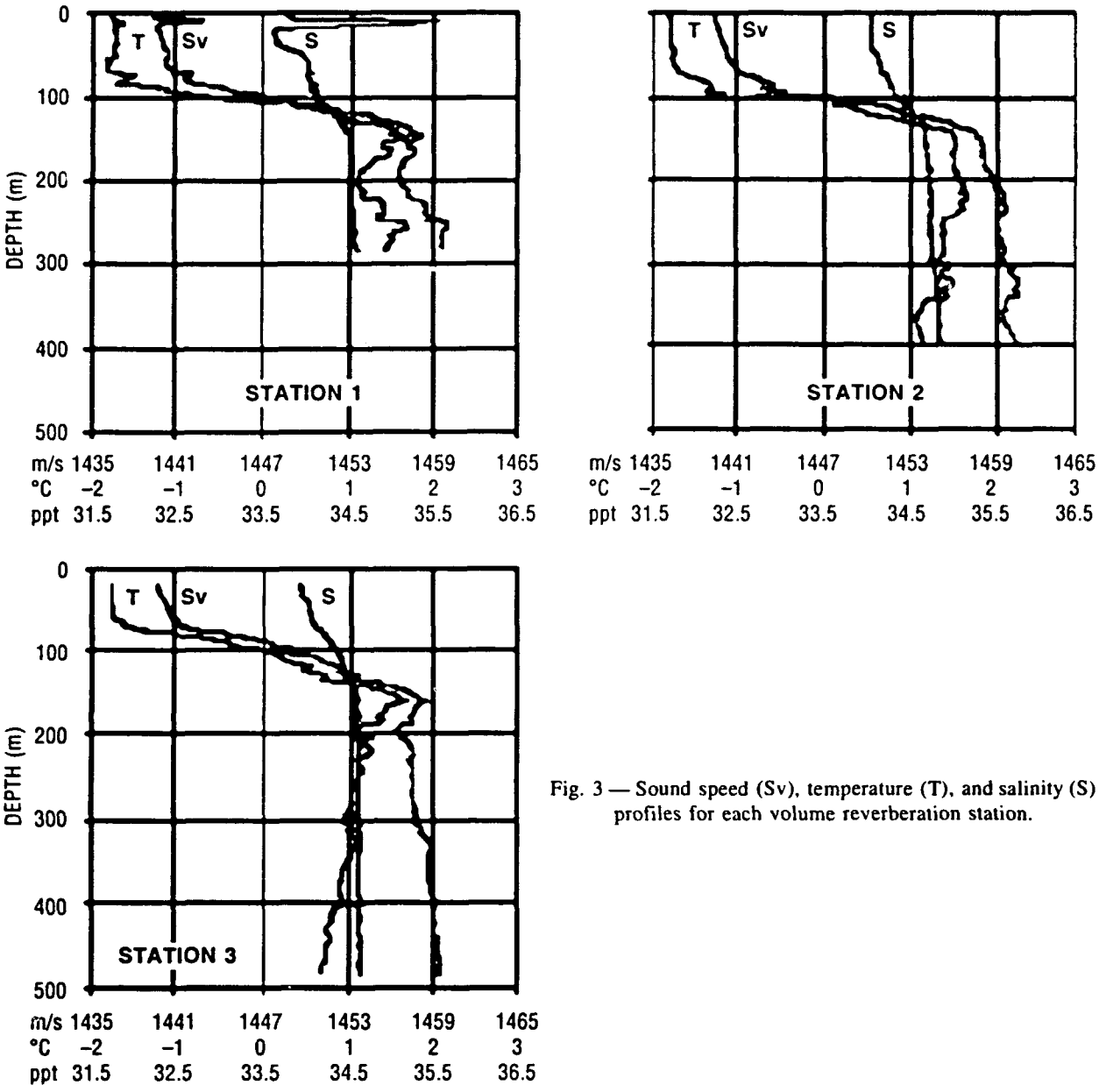

Fig. 3 — Sound speed (Sv), temperature (T), and salinity (S) profiles for each volume reverberation station.

they ranged from 14 kt to gusts of 24 kt between 1609 and 2105 on 17 May. Average windspeeds ranged from 10 to 16 kt with gusts up to 19 kt at Station 3 on 18 May [1].

Fram Strait Pelagic Food Chain

Swimbladders of fish produce resonant scattering. Peak frequencies depend on their size and depth. Near the surface, volume reverberation can also be caused by bubbles that resonate at tens to hundreds of kilohertz frequencies. The shells or bodies of zooplankton and phytoplankton can cause Rayleigh scattering at frequencies used in the MIZ 88 experiment but can cause much stronger

scattering at higher frequencies. Bubbles may become trapped in the shells of pteropods and produce resonant scattering at 30 to 50 kHz or higher frequencies in deep layers. Knowledge of the types and sizes of fish and other pelagic organisms, therefore, gives clues that help to explain the sources and the variability of volume reverberation in the Fram Strait MIZ.

Despite apparently harsh conditions, the Arctic Ocean and its MIZs are a highly productive environment that contains a variety of living organisms. Studies of food sources and predators, often easier to collect or observe, indicate that small fish are present in the Fram Strait. Phytoplankton and zooplankton, as well as the physics of mesoscale eddies, were studied as a part of MIZEX 84, a major international research program [5].

Historically, the area between Greenland and Spitsbergen has a higher population of zooplankton than areas adjacent to the USSR, Canada, and Alaska. Zooplankton rely on phytoplankton or smaller zooplankton for food [6]. Zooplankton, primarily the copepods, *Calanus hyperboreus*, *Calanus glacialis*, and *Calanus finmarchicus*, were caught at a plentiful rate of 100 to 200 per cubic meter in July 1983 in the same part of the Fram Strait where the 1988 experiment was conducted [7]. *Calanus* feed on the dinoflagellates, diatoms, and ciliates which are abundant in the Fram Strait [8]. Melting of ice in the Greenland Sea MIZ aids in the growth of these phytoplankton as do eddies and upwellings. A low ambient level of nutrients and grazing by large copepods, however, limit the abundance of phytoplankton in the Fram Strait [9].

Norwegian scientists from the University of Tromsø studied marine animals living in sea ice of the Fram Strait and western Barents Sea between 1982 and 1987. They found mainly amphipods, copepods, and polar cod (*Boreogadus saida*).* Small schools of young polar cod (only 1- and 2-year olds) were found between ice floes and in crevices of the ice. The stomach contents of these fish were mainly calanoid copepods. Polar cod, and the amphipod, *Gammarus wilkitzkii*, made up over 98% of the stomach contents of the black guillemot seabird, *Cepphus grylle*, caught in areas of multiyear ice [10].

The Institute of Marine Research in Bergen, Norway, studied Northeast Arctic cod, *Gadus morhua*, and their prey from 1984 to 1986. Their report indicates that these large fish, also known as Atlantic cod, were caught off the western coast of Spitsbergen as far north as 80°N. Deep-sea shrimp (*Pandalus borealis*), redfish (*Sebastes* spp.), polar cod, (*B. saida*) and krill (*Euphausiacea*) were among the species identified by sampling the stomach contents of these Atlantic cod [11].

B. saida is common in the Arctic Ocean, especially in MIZs [13]. *A. glacialis* is an oceanic species that has been caught mostly in the western part of the Arctic Ocean. German researchers from the Institute of Polar Ecology at University Kiel report that *A. glacialis* outnumbered *B. saida* by a factor of 10 in trawls made near the northeast Greenland coast at depths between 90 and 500 m. These catches were made during the RV *Polarstern* cruise ARK VII/2 in July and August 1990 using both Agassiz and bottom trawls. Samples were taken at latitudes from 78°N to 82°N, but

B. saida is referred to as Arctic cod in North American taxonomy texts to distinguish it from a similar polar cod species, *Arctogadus glacialis*, which is an important part of the pelagic food chain in parts of the high Arctic ocean [12]. Some European texts, however, refer to *B. saida* as polar cod. In this text, the term polar cod refers to both, and scientific names are used when a distinction between the two is needed.

mainly north of 80°N. Densities of *A. glacialis* ranged from 214 to 4789 fish per square kilometer. Their average length was 15 cm [14].

Although over 20 species of fish, including *Lycodes* spp., sculpin, and Arctic scate, have been found between Spitsbergen and Greenland, most are benthic or demersal [15] and would therefore not be seen in the upper 1000 m of the MIZ 88 site. Among the exceptions are the pelagic larvae of wolffish (*Anarchichas lupus lupus*), which hatch between January and July and grow to be 5 to 6 cm long before they join the adult fish on the bottom in late autumn [16]. Golden redfish (*Sebastes marinus*) juveniles tend to live near the shore, but larger adults may be off the coast at 100- to 1000-m depths. Deep-water redfish (*Sebastes mentella*) stay mainly offshore at depths of 300 to 910 m and are found above great ocean depths [17]. Another pelagic deep-water fish, *Rhodichthys regina*, normally lives below 1500 m. This species is worth mentioning because the deep-water MIZ 88 experiment area is part of its normal habitat, and frequent upwellings may bring them to somewhat shallower depths [18]. *R. regina* do not have swimbladders [19] but may attract predators that do into the lower extreme of the scattering depths measured. Atlantic herring, Norway pout, redfish, and capelin are found near Spitsbergen, but generally south of 79°N and east of 10°E [20]. The Greenland shark, a major predator of the benthic fish at 200 to 600 m, also eats various pelagic fishes, birds, carrion, and seals [21]. Other pelagic fish found in the Fram Strait along the western coast of Spitsbergen include haddock (*Melanogrammus aeglefinus*), saithe (*Pollachius verens*), and blue whiting (*Micromesistius poutassou*). Blue whiting school over depths of 160 to 3000 m, 30 to 400 m from the surface as far west as 2°E at 79°N [22].

During the MIZ 88 experiment, a walrus, two seals, and several polar bears were seen. Arctic mammals, such as the polar bear (*Ursus maritimus*), the harp seal (*Pagophilus groenlandicus*), the ringed seal (*Phoca hispida*), the beluga (*Delphinapterus leucas*), and the narwhal (*Monodon monoceros*) may dive very deep to catch fish, squid, and zooplankton [2]. Polar bears are good swimmers and have been seen eating fish and seals 30 mi from the nearest land or ice. Walrus, *Odobenus rosmarus*, live on rocky islands or moving pack ice of the Arctic and eat clams and mollusks [23]. The many predators of the Fram Strait fauna indicate a substantial abundance of prey, which are the probable cause of volume reverberation.

DATA ANALYSIS

After returning from the MIZ, analog data tapes were digitized by a Masscomp minicomputer. The digitized data were then processed on a VAX computer. For each ping, a file containing 750 points, including 40 points before the signal, was extracted to represent background noise plus reverberation from the upper 1000 m below the ice.

The voltage vs. time envelope was plotted for each ping. Since there was little difference between pings in the same set, 4 to 10 pings were averaged to give a representative plot for each set. The plots for the downward-looking configuration show the direct signal, followed by surface scatter of rapidly decreasing amplitude, then the volume reverberation. For the upward-looking configuration, the plots show the direct signal, the volume reverberation, and then the surface reflections.

Figures 4 and 5 show representative samples of these plots. The baseline voltage for Figs. 4 and 5 varied because gain settings and transducer characteristics changed. The top two plots in Fig. 4 show channels 1 and 2 for a 5-kHz data set. The second data channel used a higher gain than

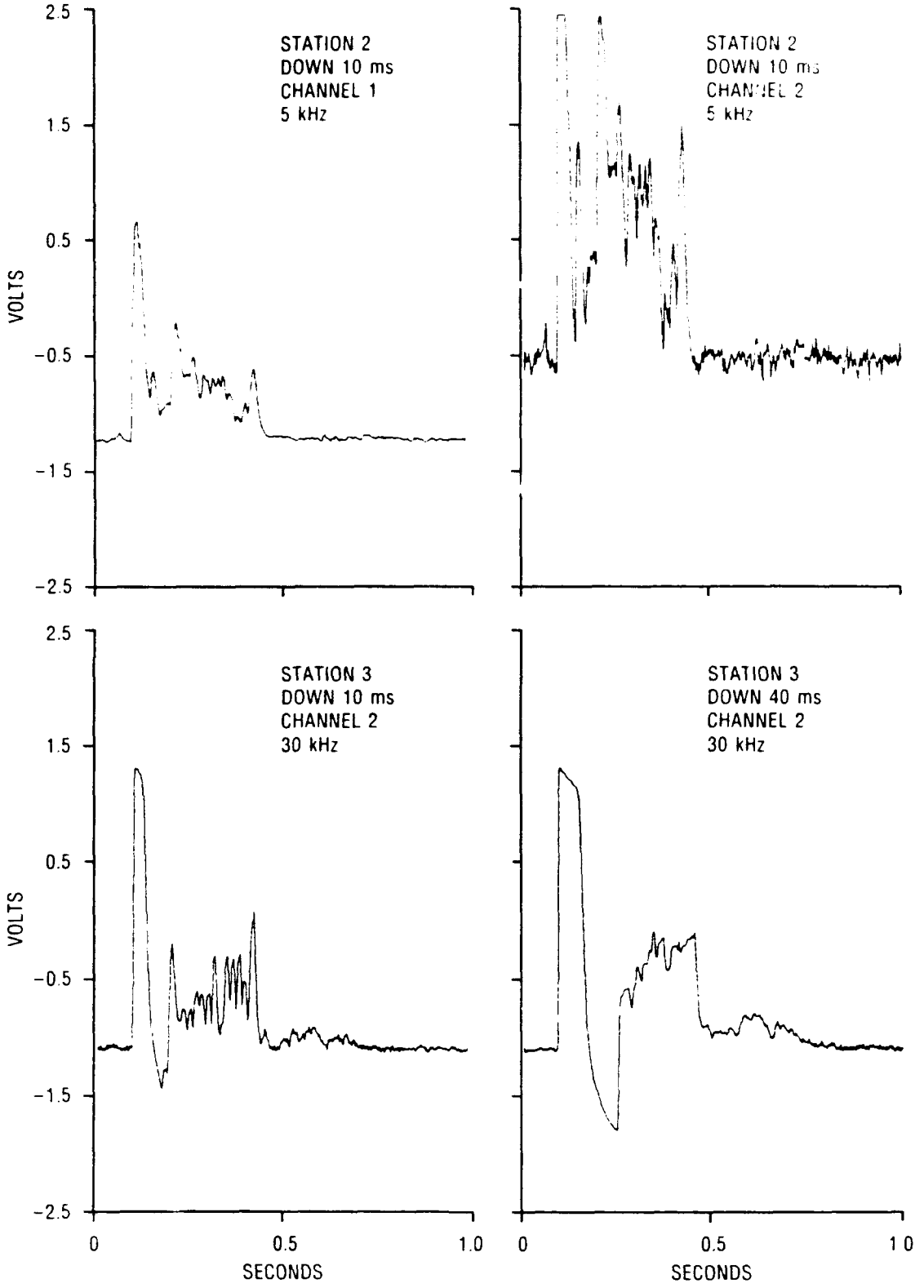

Fig. 4 — Samples of voltage vs. time plots for transducers looking down.

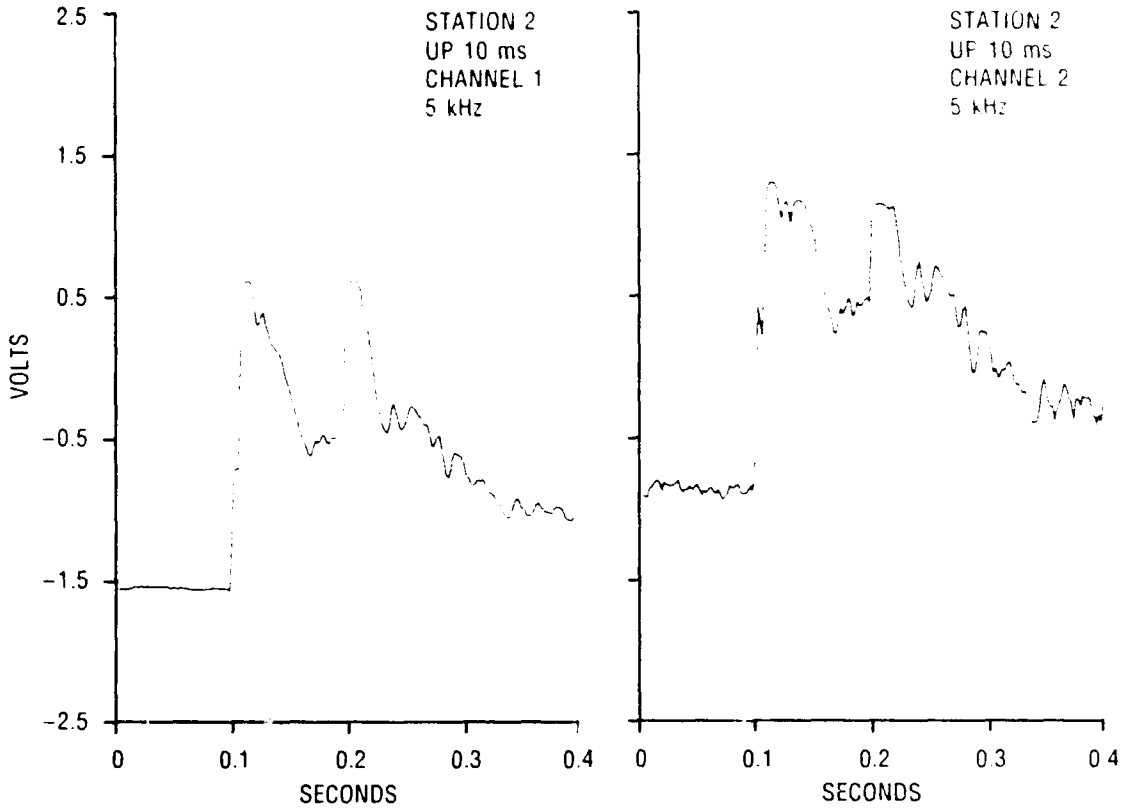

Fig. 5 — Samples of voltage vs. time plots for transducers looking up.

the first to bring out returns from deeper layers. Although deeper layers are more readily detected on channel 2, increased gain also resulted in increased noise, clipping of the direct signal, and voltage drops below the noise where strong signals overloaded the electronics. The lower two plots show that using longer pulse lengths was more effective for showing deep layers, but caused signal dropouts for the upper 50 m. Even with a 10-ms pulse length, the shallowest valid reverberation data for downward-looking transducers began at 35 m.

At Station 2, upward-looking transducers were used to measure volume reverberation in the upper water column. Samples of these data are shown in Fig. 5 with an expanded time scale to show more detail. The transducer was lowered to 65 m for 3.5, 5.0, 7.5, and 12.0 kHz measurements. The direct part of the signal and noise due to transition from transmit to receive modes left only 20 to 25 m of data before the surface return for the 65-m transmitter depth.

Volume scattering strength as a function of depth was obtained from the average voltage envelope vs. time plots using an equation derived from Urick (1975):

$$Sv = 20 \log V - SL - FFVS - 10 \log m - 10 \log(1 - \cos(b/2)) + 20 \log t + act - \text{Gain} + 20.8 , \quad (1)$$

where Sv is volume scattering strength, V is voltage level of the received signal, SL is source level, $FFVS$ is free-field voltage sensitivity of the transducer, m is pulse length, b is the -3-dB beamwidth,

t is time in seconds, a is the frequency-dependent attenuation coefficient, c is sound speed, and the constant 20.8 is a combination of factors related to the geometry [24]. The data sampled before the ping began was used as the noise threshold to optimize the tradeoffs between missing weak signals and seeing numerous noise spikes. Some of the pings have noise spikes that were too strong to be totally eliminated by averaging pings. Due to the time factor in the equation, the plots are increasingly sensitive to noise with depth and deep erratic returns are mostly from noise; therefore, volume scattering levels are not dependable at depths where the plots show large frequent variations with depth.

By integrating the scattering strengths over the selected depth intervals, a layer strength was calculated for each layer. Layer depth ranges were chosen with reference to the depths of the thermocline and the bottom of the AIW layer and are similar for all frequencies at a given station at the same time of day. Layer boundaries are approximate, since scattering layers change gradually and two layers may overlap. Scattering strength integrated over all the depths between the top of the shallowest layer and the bottom of the deepest layer of interest in the water column gave the column strength for each frequency and station.

RESULTS

Results include the volume scattering strengths as functions of depth for each frequency at each station, along with integrated layer strengths and column strengths. Data from both channels are included for Station 1 in Figs. 6 and 7 to show how they compare at each frequency. The increase in gain on channel 2 increases the signal amplitude so that the direct signal is more likely to overload the electronics and cause shallow reverberation returns to drop out on that channel. In Figs. 8 and 9, therefore, only channel 1 is shown for each case, unless channel 2 brought out the reverberation layers better. Figure 10 shows layer strengths as a function of frequency. Levels for the three stations are compared for surface layers, layers in the thermocline, layers below the thermocline to 300 m, and layers deeper than 300 m, as well as for very deep layers starting at 800 m for Station 1 and 600 m for Station 3 to a maximum of 1000 m deep. Station 2 had no strong scattering below 800 m.

Scattering Strength vs. Depth

The three parts of Fig. 6 show volume scattering strengths vs. depth for the 10-ms pulses from Station 1. Figure 6a shows both channels for 3.5, 5.0, and 7.5 kHz. At these frequencies there is a strong layer in the colder water above the thermocline, another layer that extends from 100 m to around 300 m, low levels of reverberation between 400 and 800 m, and a deep layer. The shallow layers are stronger and cover a wider depth range at 5.0 and 7.5 kHz than at 3.5 kHz. The upper scattering layers at 7.5 kHz extend from 35 to 575 m. At both 7.5 kHz and 3.5 kHz the deep layer extends from 875 to 1000 m but it is about 15 dB stronger, –70 dB at 3.5 kHz. This layer starts about 900 m and is very weak at 5 kHz. Above 7.5 kHz, noise masks any reverberation from below 600 m for 10-ms pulses. Figure 6b shows data for 16 and 20 kHz. The scattering layers cover the water column from 70 m to about 600 m. The strongest scattering between 100 and 300 m is about 20 kHz. The peak scattering strength at 20 kHz is about 5 dB higher than that at 16 kHz. In the 500-m layer, the maximum reverberation occurs closer to 16 kHz. Figure 6c shows the scattering strength profiles for 25 and 30 kHz. At 25 kHz, the volume reverberation is a little weaker and does not go as deep as that for 20 kHz. The layers are no longer contiguous at 30 kHz and extend to only 545 m, unlike the low-gain channel 1 of the 25-kHz data, which has contiguous layers from 75 m to 720 m and becomes increasingly noisy below 600 m.

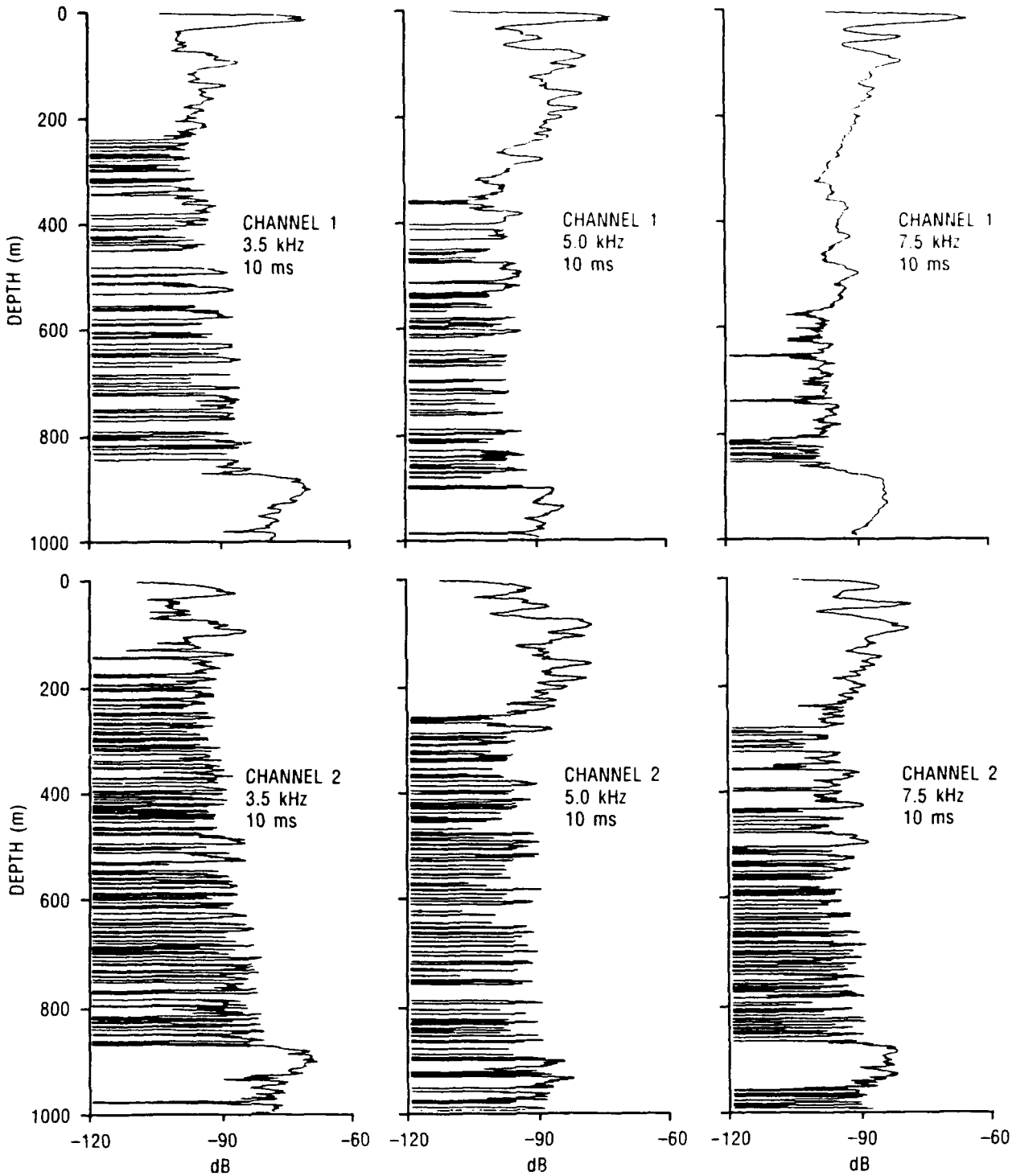

Fig. 6a — Station 1: Scattering strength vs. depth for 10-ms pulses at 3.5, 5.0, and 7.5 kHz.

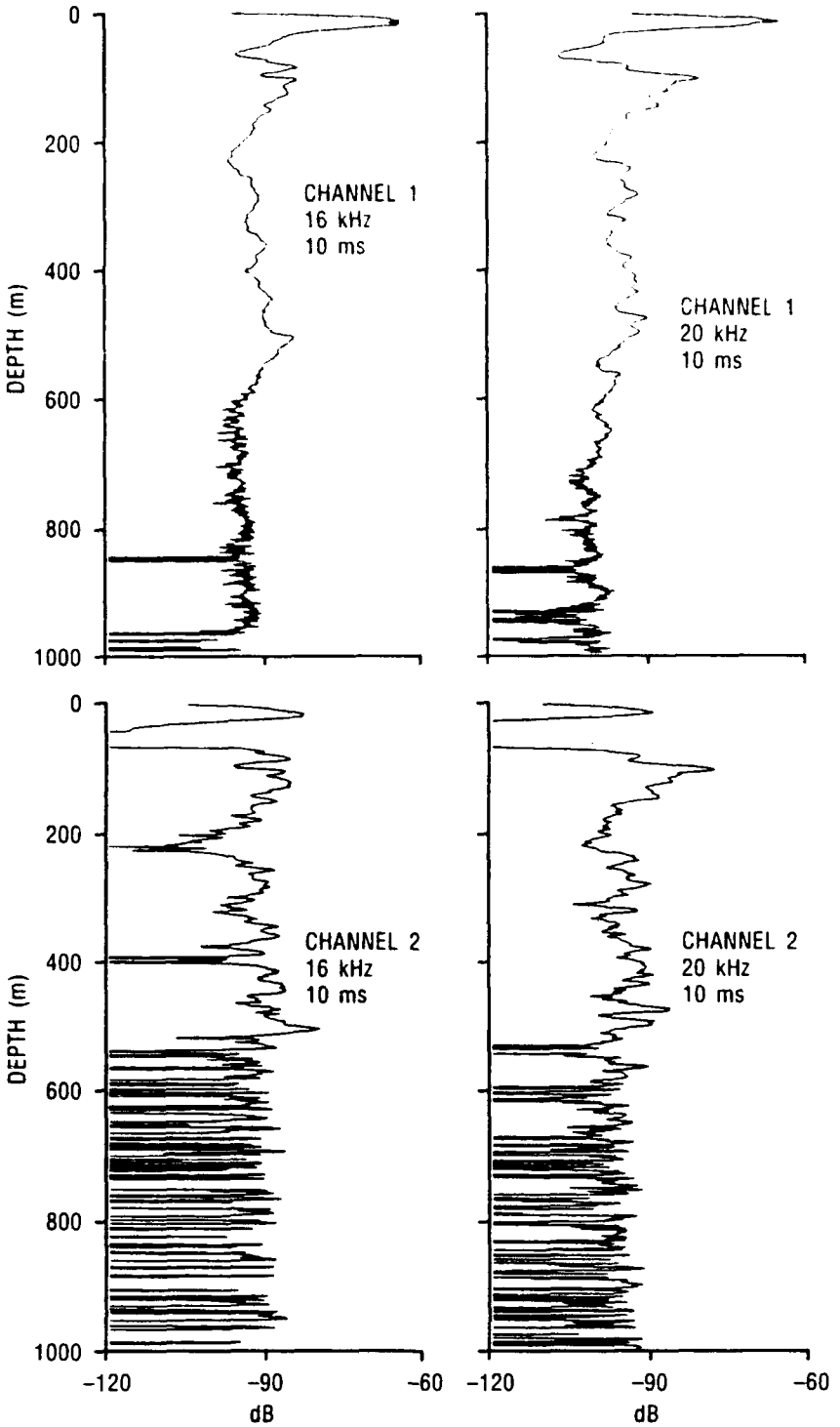

Fig. 6b — Station 1: Scattering strength vs. depth for 10-ms pulses at 16 and 20 kHz.

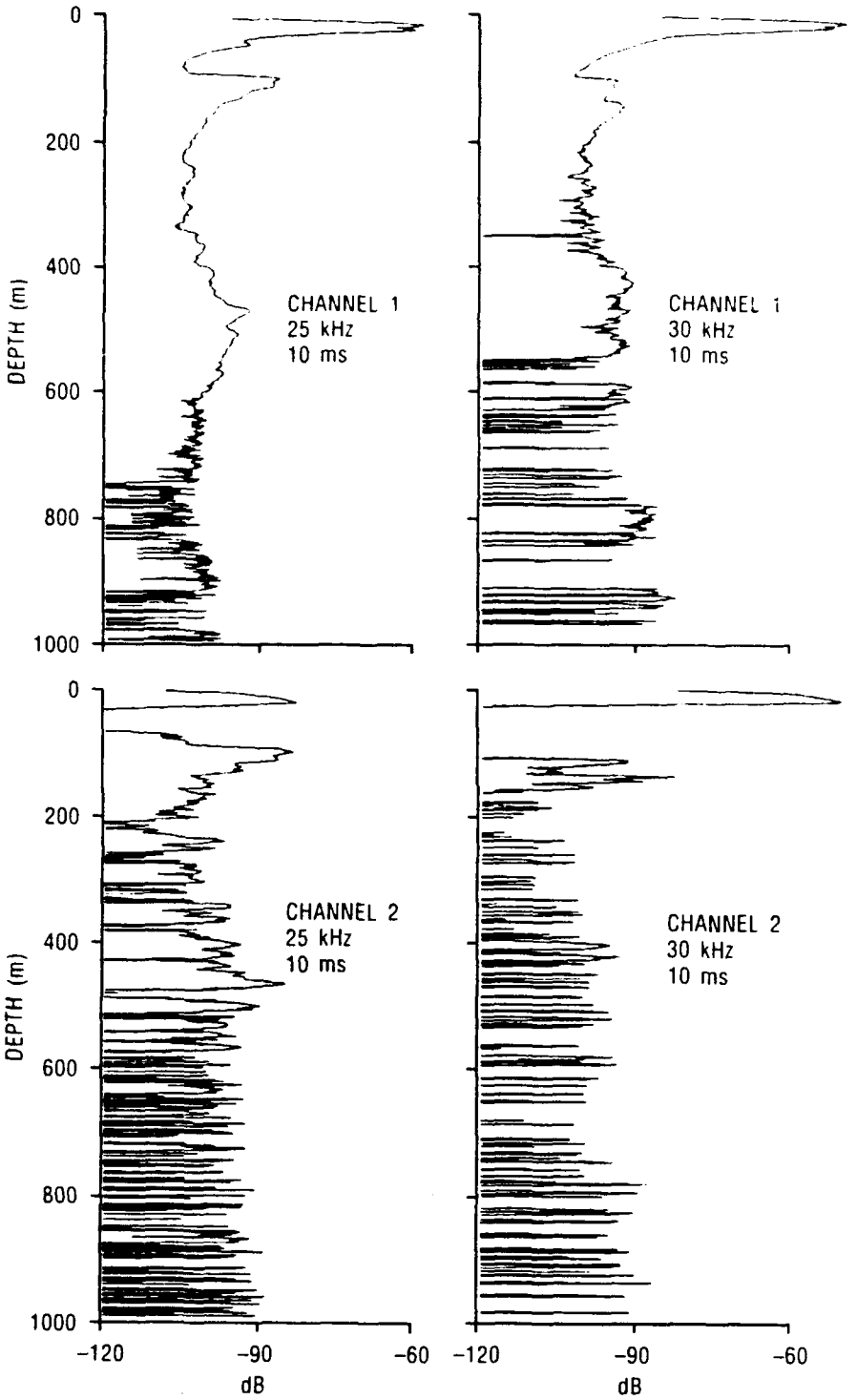

Fig. 6c — Station 1: Scattering strength vs. depth for 10-ms pulses at 25 and 30 kHz.

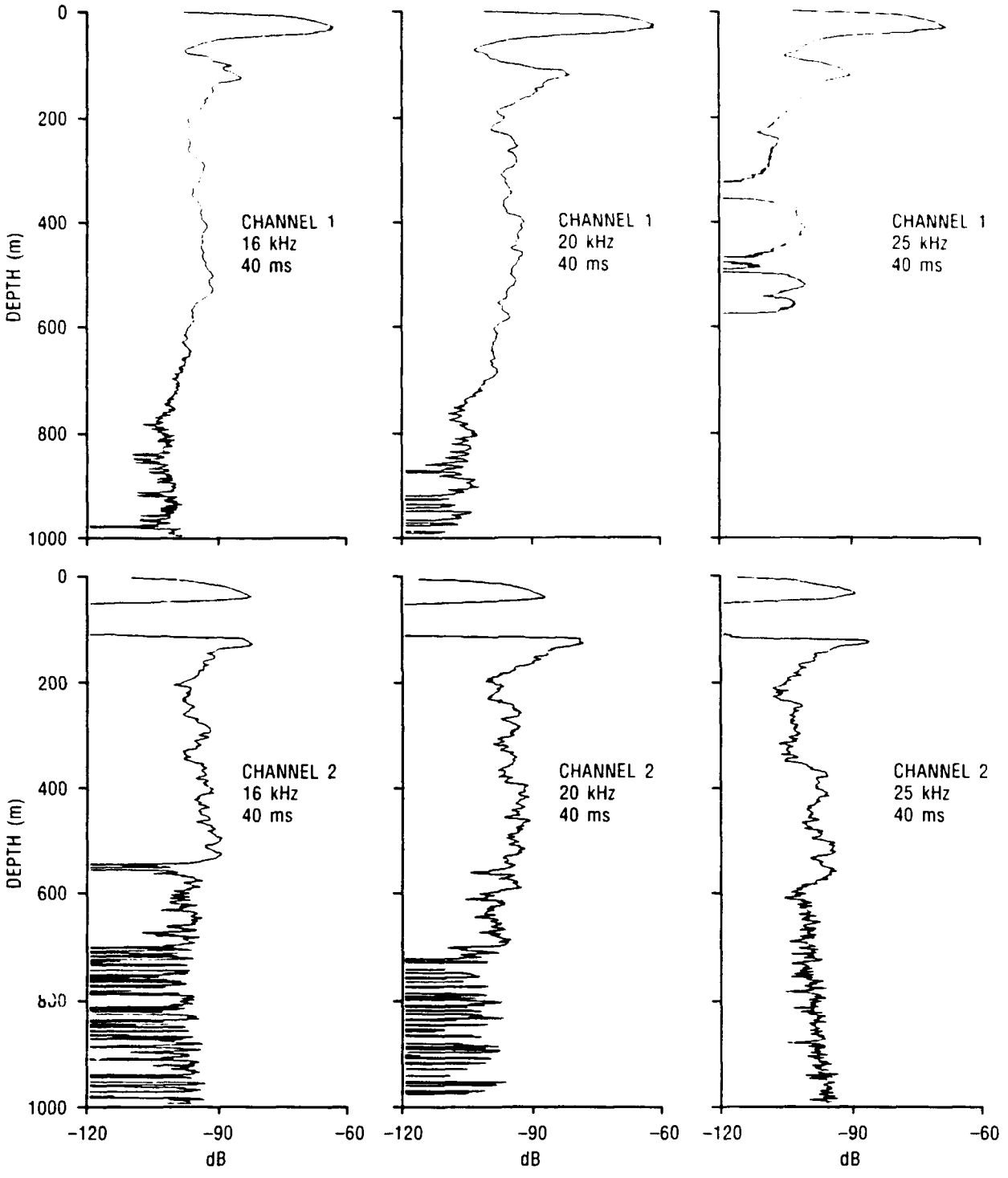

Fig. 7a — Station 1: Scattering strength vs. depth for 40-ms pulses at 16, 20, and 25 kHz.

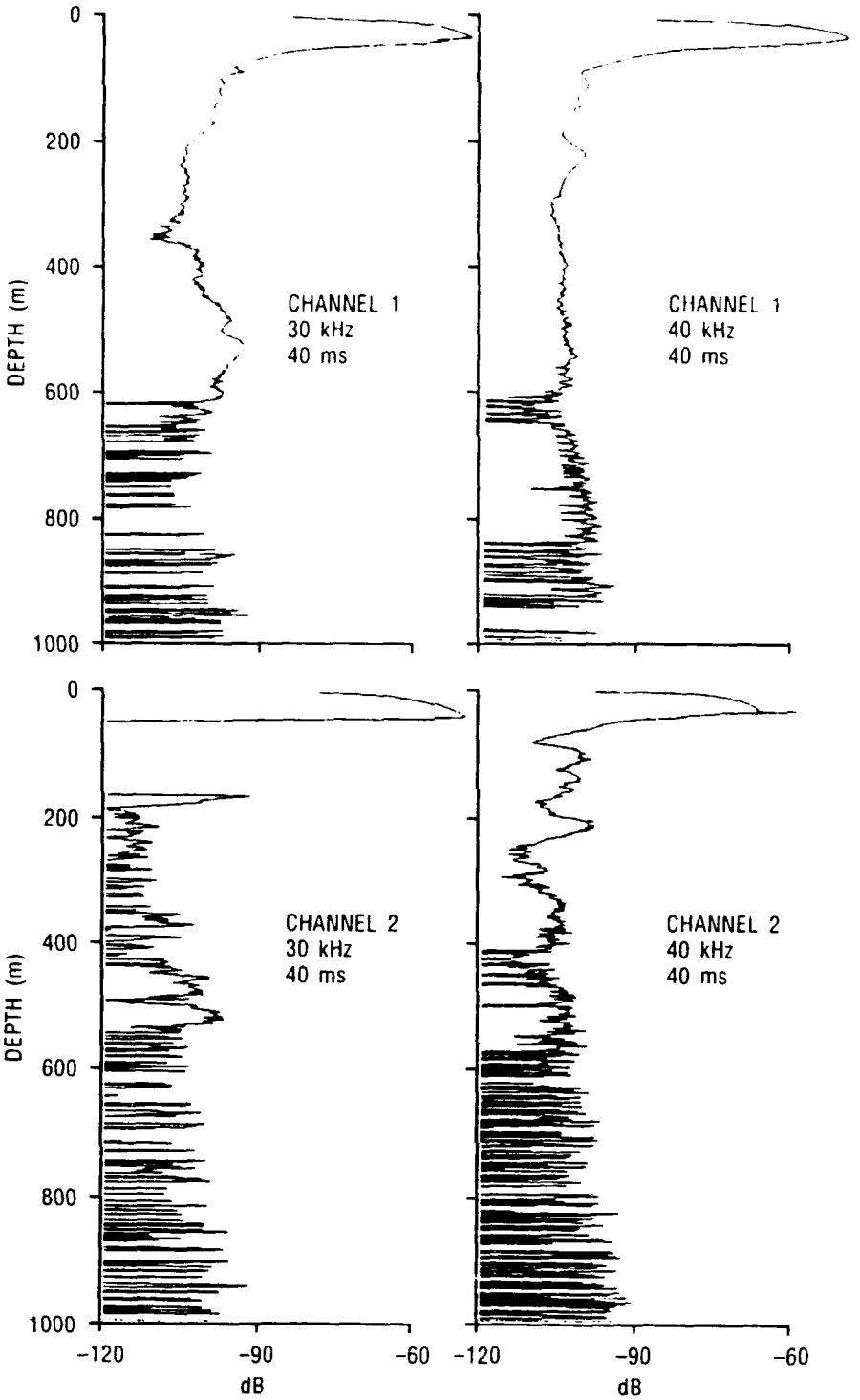

Fig. 7b — Station 1: Scattering strength vs. depth for 40-ms pulses at 30 and 40 kHz.

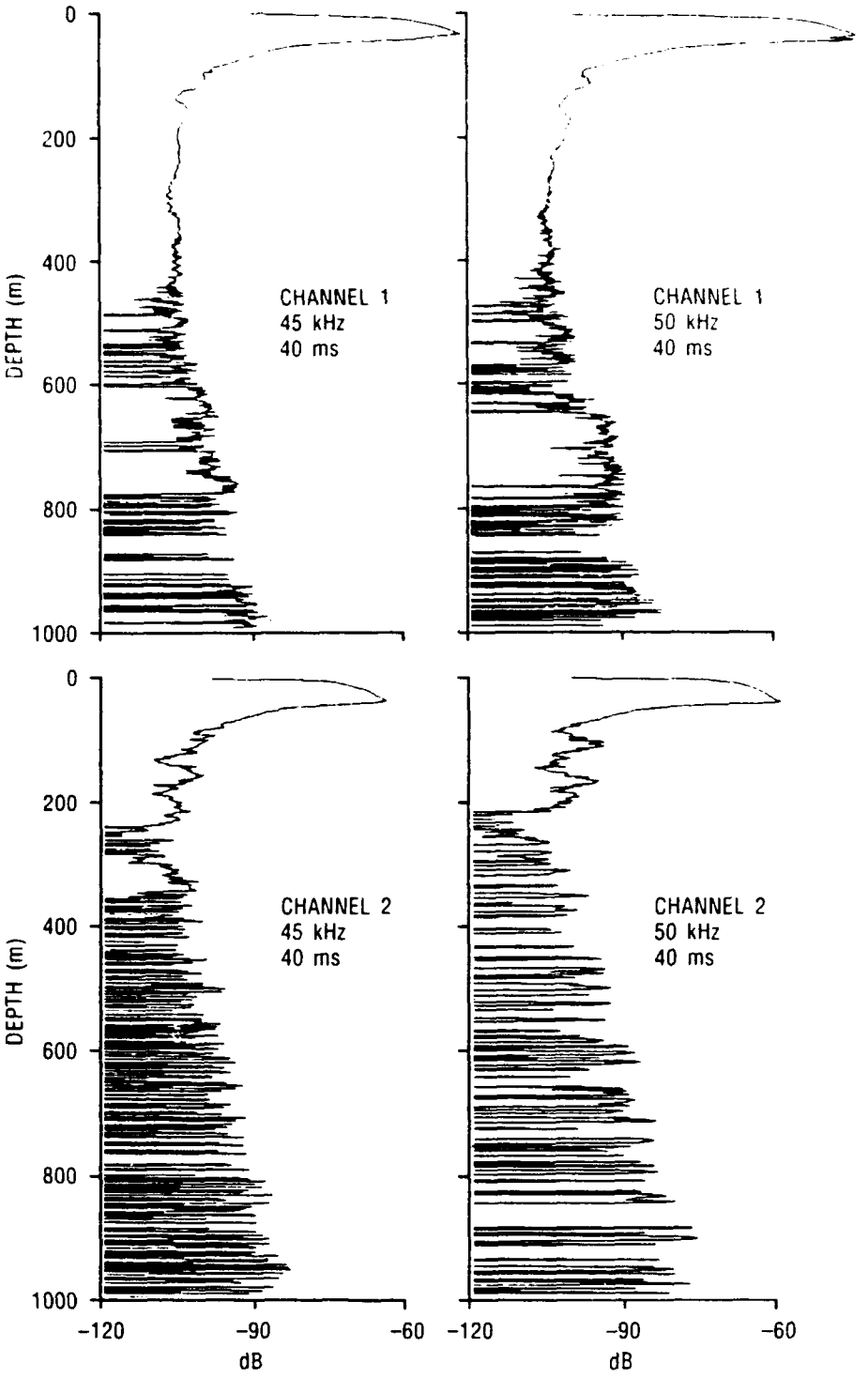

Fig. 7c — Station 1: Scattering strength vs. depth for 40-ms pulses at 45 and 50 kHz.

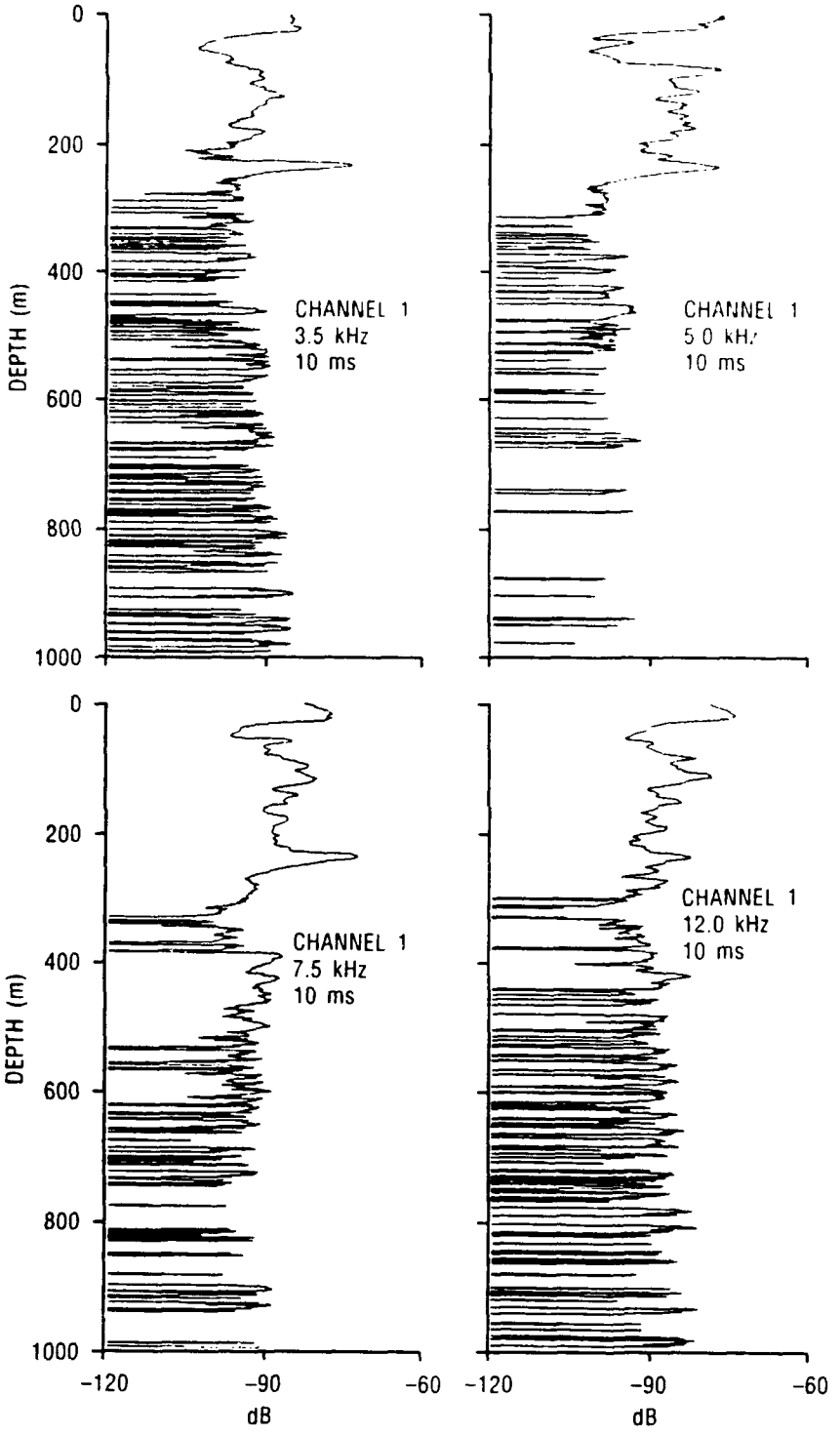

Fig. 8a — Station 2: Scattering strength vs. depth for 10-ms pulses at 3.5, 5.0, 7.5, and 12.0 kHz.

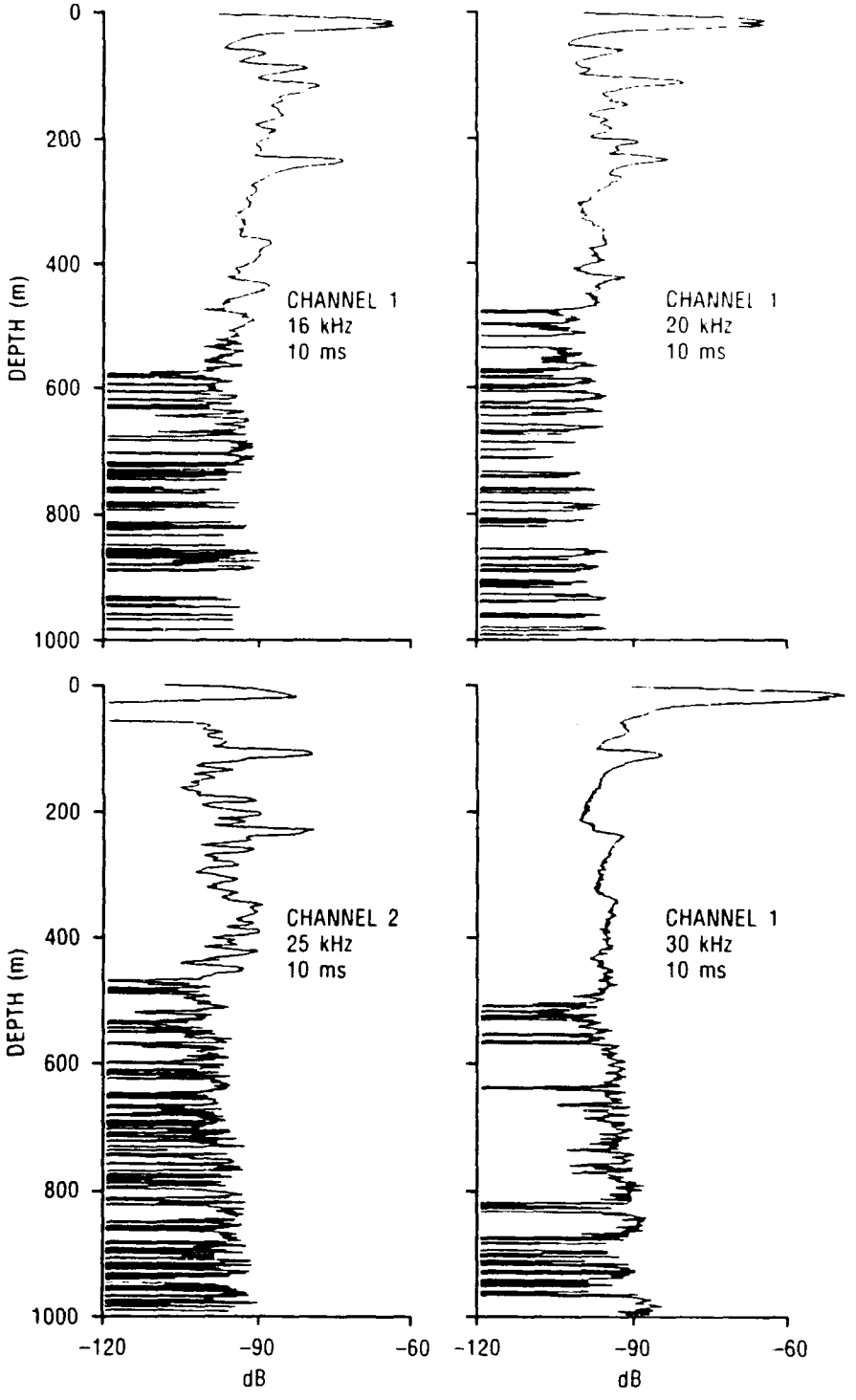

Fig. 8b — Station 2: Scattering strength vs. depth for 10-ms pulses at 16, 20, 25 and 30 kHz.

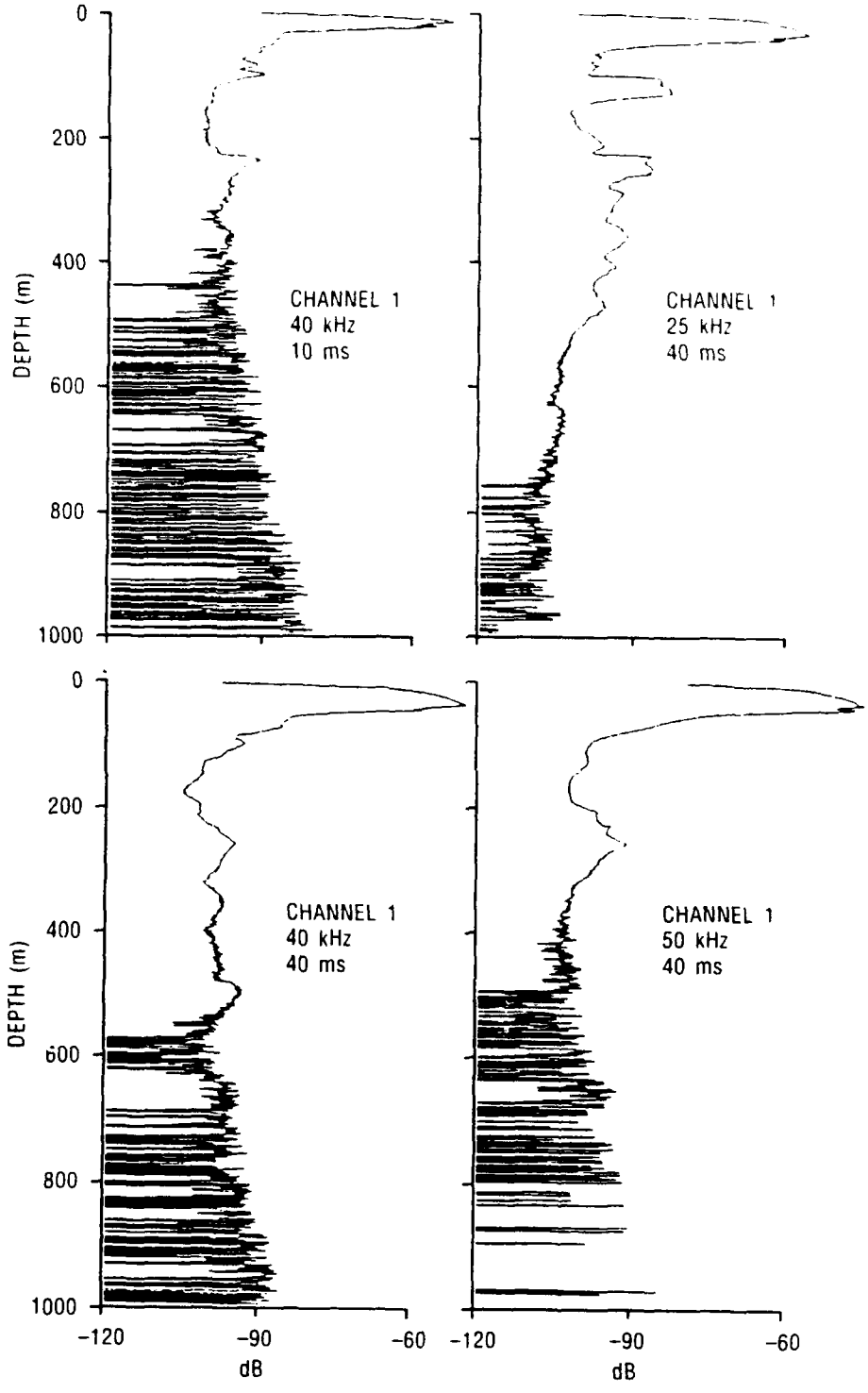

Fig. 8c — Station 2: Scattering strength vs. depth at 25, 40, and 50 kHz.

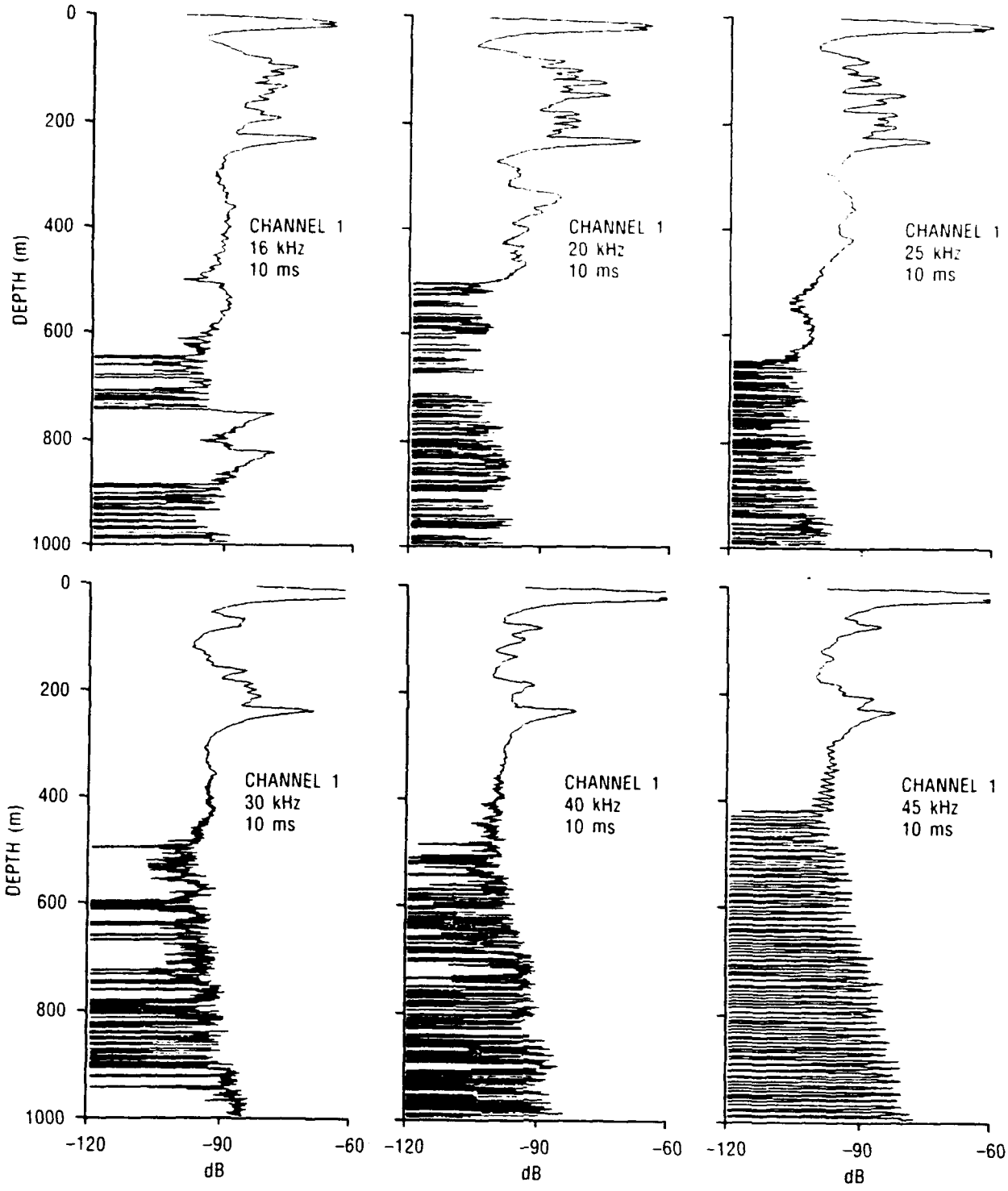

Fig. 9a — Station 3: Scattering strength vs. depth for 10-ms pulses.

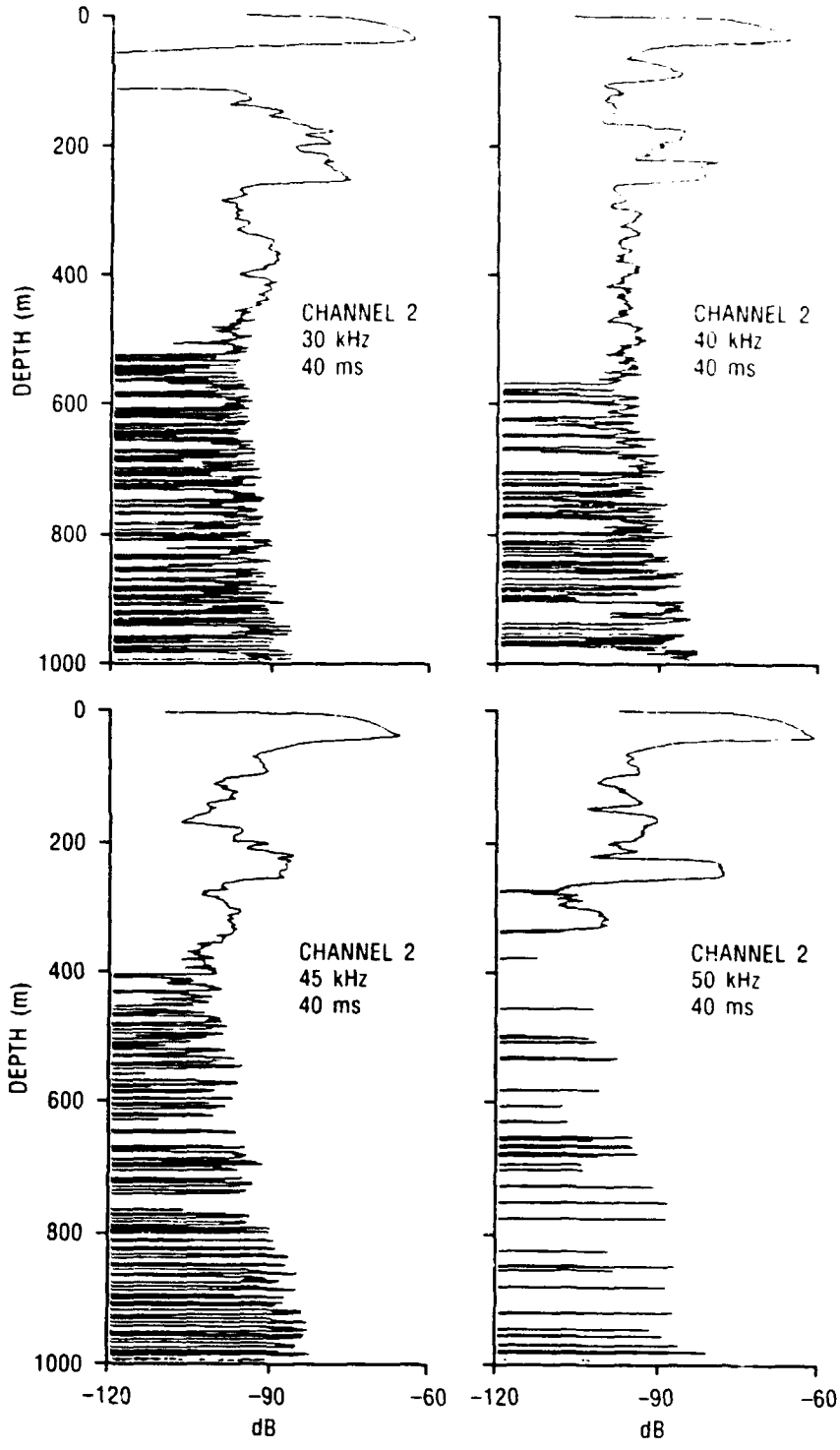

Fig. 9b — Station 3: Scattering strength vs. depth for 40-ms pulses.

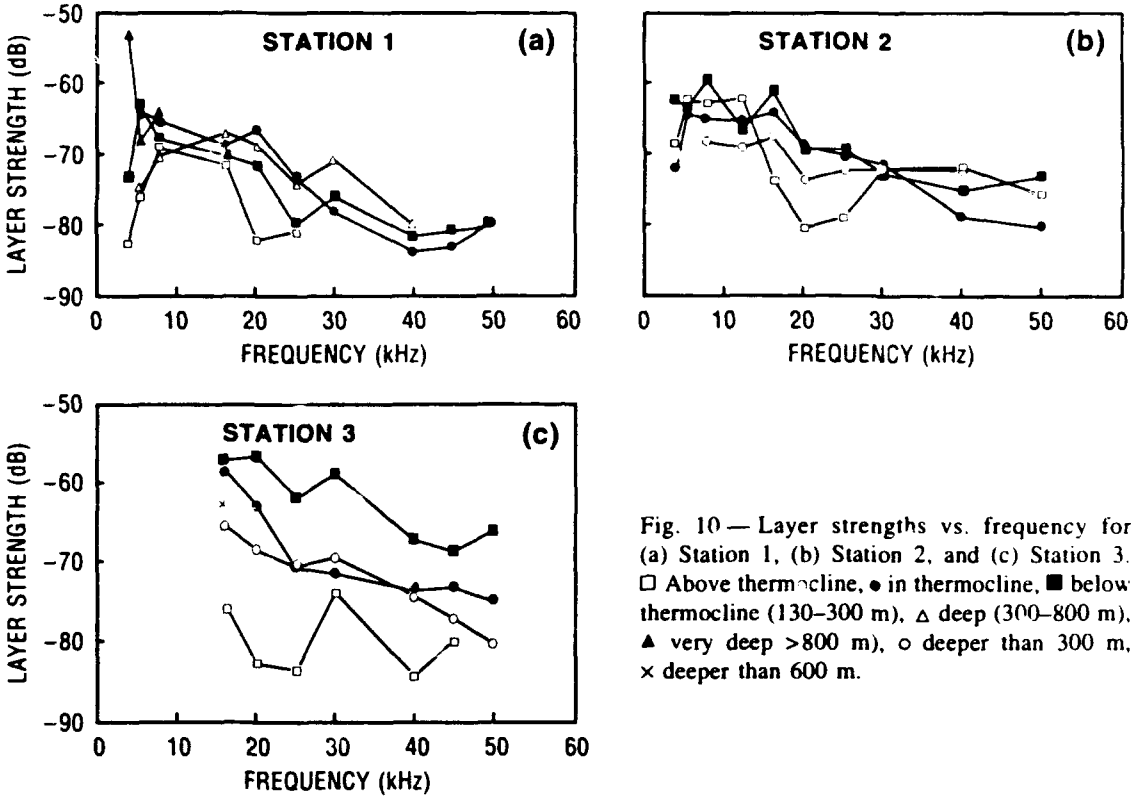

Fig. 10 — Layer strengths vs. frequency for (a) Station 1, (b) Station 2, and (c) Station 3. □ Above thermocline, • in thermocline, ■ below thermocline (130–300 m), △ deep (300–800 m), ▲ very deep >800 m), o deeper than 300 m, × deeper than 600 m.

Figure 7 shows volume scattering strength vs. depth for 40-ms pulses from Station 1. Figure 7a includes data for 16, 20, and 25 kHz. The data sets for 16 and 20 kHz show volume reverberation layers throughout most of the 1000-m depth range. Below 600 m, noise contaminates the data at 16 kHz. The noise is not apparent in channel 1 of the 20-kHz data until below 700 m. At 25 kHz, returns from deeper layers are weak and in the low-gain channel 1, layers are not contiguous and end above 600 m. In the high-gain channel 2, the signal dropout following the direct pulse is quite pronounced and there is a lot of noise below 600 m. Figure 7b shows data for 30 and 40 kHz. The 30-kHz volume reverberation was clearly divided between a layer from about 80 to 200 m and a large layer centered around 500 m depth. At 40 kHz, channel 1 shows a weak continuous layer down to 600 m that begins to be contaminated with noise below 300 m. Channel 2 shows more separation between shallow layers and noise below 400 m. Figure 7c shows scattering strength vs. depth for 45- and 50 kHz pings. The plots for these two frequencies are quite similar, especially above 400 m, with scattering levels a little higher than –100 dB until they fade into the noise. The high-gain channel seems to indicate that returns deeper than 250 m are mainly noise at these frequencies.

In Fig. 8a, the Station 2, channel 1, upward- and downward-looking 10-ms pulse length data for each frequency between 3.5 and 12.0 kHz has been combined. Removing the direct part of the downward-looking data and replacing it with the reverberation part of the upward-looking data set gives a picture of the scattering strengths over the entire upper 1000 m of the water column. A strong layer was seen near the surface. At 3.5 kHz scattering strength is –83 dB near the surface. Between 75 and 200 m it peaks at –88 dB, and at 240 m there is a thin layer with a scattering

strength of –71 dB. Temperature vs. depth profiles for Station 2 show the water temperature increasing to 0°C at 100 m and as high as 1.6° below. The scattering strength also increases dramatically at that depth. The large spike at 240 m corresponds to the temperature maximum shown in Fig. 3. The data become too noisy below 300 m. At 5 kHz the near-surface reverberation strength is –75 dB. The layer between 75 and 200 m peaks at –77 dB. The layer between 200 and 275 peaks at –78 dB. There may be a weak layer between 450 and 500 m at 5 kHz. At 7.5 kHz the three upper layers have scattering strengths of –77, –80 and –72 dB, respectively. At 7.5 kHz the scattering is almost a continuous layer from 275 to 625 m but becomes noisy below 500 m. At 12 kHz the near-surface returns peak at –74 dB. The 75- to 200-m layer peaks at –79 dB. The 200- to 275-m layer is less distinguishable from the layer above it and peaks at –83 dB. Between 300 and 450 m the peak scattering strength is –83 dB.

Figure 8b shows one channel from each of the 10-ms pulse length data files at 16, 20, 25, and 30 kHz. The scattering layers covered most of the upper 500 m for all four frequencies with layers of strong reverberation around 100 and 250 m. This is just above and below the depth of the main layer from Station 1. The returns at 30 kHz below 550 m are almost continuous but are contaminated with noise as strong or stronger than the reverberation.

Figure 8c shows data from Station 2 for 25, 40, and 50 kHz for 40-ms pulse length sets. Data for 10-ms pulse length at 40 kHz are also shown. The longer pulse length caused the layers to appear to be in a larger depth range. Comparing the 25- and 40-kHz data sets shows that the 40-ms pulse was able to insonify the weak deeper layers, which were too noisy using the 10-ms pulse length. Both show the layers at 110 and 250 m. At 40 kHz the layer around 500 m is strong for 40 ms but is hidden in the noise for 10-ms pulses. The 50-kHz data in Fig. 8c show a distinct peak around 250 m, but the peak around 100 m is weaker than at 40 kHz.

Station 3 data are shown in Figs. 9a and 9b. Figure 9a shows one channel from each frequency of 10-ms pulses. The lowest frequency sampled at this station—and the only one to show a strong scattering layer below 750 m—was 16 kHz. The 16-kHz profile also showed strong scattering between 100 and 275 m, similar to that at Station 2, and a weak 500- to 600-m layer. The 20- and 25-kHz data showed reverberation levels staying less than –100 dB and in the noise below 500 m. Intermittent noise spikes, such as those below 500 m at 30, 40, and 45 kHz, indicate that the signal-to-noise ratio was too low to give valid reverberation results. Figure 9b shows the 40-ms scattering strength data for 30 to 50 kHz. In these plots the main scattering layers are between 70 and 300 m. The layer around 250 m was weaker at 40 and 45 kHz than at 30 and 50 kHz in Fig. 9b. In general, the maximum depth of distinct layers decreased gradually with frequency from 25 to 50 kHz. Otherwise, the scattering strength plots looked similar from one frequency to the next.

Layer and Column Strengths

Figures 10a to 10c compare layer strength vs. frequency for all layers at the same station. At 25, 30, and 40 kHz, there was less than 3-dB difference between corresponding 10- and 40-ms data, with less than 1 dB in many cases. For small differences between channel 1 and channel 2 and between 10- and 40-ms pulses, decibel values were averaged.

Scattering strength vs. depth (Figs. 6 to 9), and the Fig. 3 temperature profiles were used to determine the depth ranges of scattering layers shown in Fig. 10. The shallow layers were divided according to their relationship to the steep thermal gradient, which began between 70 and 90 m and ended between 120 and 160 m. All but the higher frequency cases, where signal dropouts and the 40-ms direct pulse obscured it, had a layer above the thermocline. Depths within the thermocline

were a separate layer. The AIW layer below the thermocline extended to between 300 and 400 m. Layers were divided corresponding to minimums in the scattering strength below that. Scattering strengths dropped into the noise at different depths for each scattering strength profile, but always above 800 m. Only the three lowest frequencies on Station 1 and 16 kHz at Station 3 had good scattering data below 800 m.

Figure 10a shows layer strength vs. frequency for Station 1. The layer above the thermocline peaks between 7.5 and 16 kHz in the –70-dB range. Data do not show scattering strengths above the noise in the upper layer for frequencies above 25 kHz at Station 1. The frequency dependence in the thermocline has a –64-dB peak at 5 kHz and –67 dB at 20 kHz. Values decrease to –84 dB at 40 kHz then increase to –80 dB at 50 kHz. The water column below the thermocline down to 300 m has a distinct peak at 5 kHz and a large dip at 25 kHz. The deep layer, between 300 and 800 m, peaks at 16 and 30 kHz with levels of –67 and –71, respectively. The very deep layer is very strong: –53 dB, at 3.5 kHz, about –68 dB at 5 kHz, and –64 dB at 7.5 kHz.

Figure 10b presents layer strength data for Station 2. The layer above the thermocline is 6 dB or more stronger than that for Station 1 primarily because scattering from the upper 35 m obtained using the upward-looking transducer is included. It levels out between 5 and 12 kHz around –62 dB. It decreases to –80 dB at 20 kHz and increases to –72 dB at 30 and 40 kHz, then decreases to –76 dB at 50 kHz. In the thermocline, the layer strength is –65 dB for the 5- to 16-kHz data. It then decreases to –71 dB at 30 kHz and –80 dB at 50 kHz. The layer starting below the thermocline varies between –60 and –70 dB in a saw-toothed pattern from 3.5 to 20 kHz. This layer decreases to –75 dB at 40 kHz and rises to –73 dB at 50 kHz. A layer deeper than 300 m is shown for frequencies from 7.5 to 40 kHz. It is about –69 dB for 7.5, 12, and 16 kHz then dips to –74 dB at 20 kHz and slowly rises to –72 dB at 40 kHz.

Figure 10c shows the layer strengths for Station 3. Layer strengths above the thermocline are –75 dB at 16 kHz, around –83 dB for 20 and 25 kHz, up to –74 dB at 30 kHz, down to –85 dB at 40 kHz and higher again at –80 dB for 45 kHz. In the thermocline levels decrease rapidly from –58 dB at 16 kHz to –71 dB at 25 kHz, and slowly decrease from –70 to –75 dB as the frequency increased to 50 kHz. Below the thermocline down to 300 m the layer strength is about –56 dB at 16 and 20 kHz, drops to –61 dB at 25 kHz, is –58 dB at 30 kHz and between –66 and –68 dB for the higher frequencies. For the layer from 300 to 600 m, layer strength decreased gradually from –65 dB at 16 kHz to –80 dB at 50 kHz, with a small rise to –69 dB at 30 kHz. At 16 kHz there is a –62 dB layer below 700 m.

Figure 11 shows the column strength of the upper 800 m for each frequency at each of the three locations in the Fram Strait. Volume reverberation levels are higher for all frequencies at Station 3, where the column strength is –54 dB at 16 kHz and –55 at 20 kHz. It is –60 dB at 25 kHz, –58 dB at 30 kHz, and between –65 and –66 dB for the 40- to 50-kHz range. At Station 2 column strengths are between –57 and –62 dB for frequencies below 20 kHz, with a maximum at 7.5 kHz, then they drop to –65 dB at 20 and 25 kHz and gradually decrease with frequency to –70 dB at 50 kHz. Column strengths for Station 1 are lower than those for Station 2, except at 20 kHz where Station 1 data is a few decibels higher. At Station 1, total column strength for the upper 800 m at 3.5 kHz was only –70 dB. The maximum level is –60 dB at 5 kHz, decreases to –64 dB at 20 kHz, and then drops to –70 dB at 25 and 30 kHz. The column strength is –77 dB for 40 and 50 kHz and is –79 for 45 kHz.

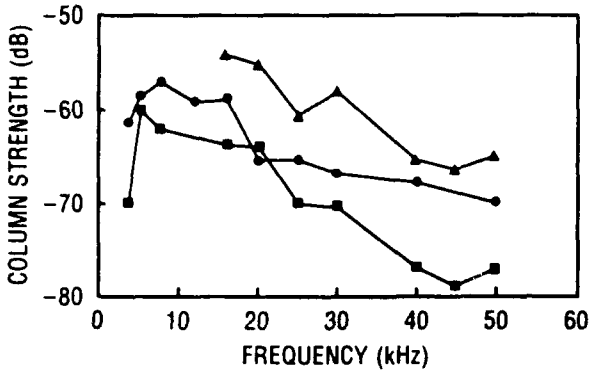

Fig. 11 — Column strength vs. frequency for surface to 800 m in the Fram Strait MIZ. ■ Station 1, • Station 2, and ▲ Station 3.

DISCUSSION

Knowledge of the biological inhabitants of the experiment area is important because the number, depth, type, and size of scattering organisms determine the magnitude and frequency of volume scattering. Other cold-water regions probably have marine biology similar to that in the Fram Strait. In a 1966–68 experiment, Hansen and Dunbar [25] collected samples of biological scatterers in the Beaufort Sea gyral. Trawls at the interface between polar surface water and underlying intermediate waters in the Beaufort Sea produced few fish but did produce numerous *Spiratella helicina*, which are small, calcareous-shelled, planktonic snails. Individual adult snails were less than 1 mm in diameter, which is about one-tenth of the size of the same species found in subarctic waters. Evidence indicated that Rayleigh scattering from the shells and exoskeletons of large aggregations of these pteropods were the cause of a thin acoustic scattering layer seen by a 100-kHz depth sounder at a 50-m depth. This layer occurred at the interface between the upper Arctic water and the Arctic intermediate water, where there is an abrupt temperature and salinity increase similar to that in the Fram Strait. A rapid change in density, and resulting sound speed, between water masses in the ocean may also be seen in sonar echo data like that collected in the Beaufort Sea. Some animals congregate around such boundaries, so that one or both mechanisms may be the cause of an acoustically detected layer, depending on frequency, amount of difference between the sound speeds in the water masses, and the numbers of fish and nekton in the area. Daily splitting and migration of the scattering layer in the Beaufort Sea, along with characteristics of the thermal discontinuity and the high frequency at which scattering was observed, indicated that the layer was not a reflection from the sound speed discontinuity.

At the lower end of the MIZ 88 frequency range, scattering of sound within the ocean volume is typically dominated by fish. Deeper, more diffuse, scattering layers evident from Beaufort Sea echograms at both 12 and 100 kHz were attributed mostly to the polar cod, *A. glacialis*, and possibly to *B. saida*, which were also caught in that study [25].

Studies of sound scattering fish in the Barents Sea indicate that young redfish, polar cod, and Northeast Arctic cod should be in the area west of Spitsbergen in May. Redfish are concentrated between January and April south of Spitsbergen. From April to June they release larvae into the waters of the Norwegian Basin. In May, June, and July, numerous young fish are found over deep water in the West Spitsbergen Current. Adult redfish, however, usually migrate northeast into the Barents Sea and by July may be in warm currents as far north as 76°N, near the Polar Front in the Barents Sea. Polar cod prefer water with temperatures from −1.7 to −1.0°C, such as that in

and above the thermocline in the Fram Strait, but may be found at any depth. They spawn from December to January in the southeast Barents Sea and off Spitsbergen, often under the ice. Afterward, they spread to the north and the east and by summer they are feeding in the Arctic Basin [26]. The polar cod population in the Barents Sea and their occurrence in the Spitsbergen area were increasing according to surveys taken from 1982 to 1986. Age and size distributions indicate that 1-year-old polar cod are 4 to 12 cm long while 2- to 5-year olds are 10 to 25 cm long. Stocks west of 30°E contained mainly younger polar cod [27].

In a 1972 experiment in the Chukchi Sea, data were taken at 38 kHz and 105 kHz. Even after eliminating 38-kHz data within 12 m of the surface because of interference from the ship's hull or bubbles caused by the ship, the two frequencies had nearly equal scattering strengths at the same location. Biological sampling during this experiment showed a large concentration of copepods, which normally produce Rayleigh scattering at these frequencies, so that one would expect about 18 dB less scattering strength from typical plankton at 38 kHz than at 105 kHz. Next to a few fish, including polar cod and sculpin, euphausiids were the best acoustic scatterers caught. Larger fish could not be caught with the method used. After considering several possible explanations, bubbles attached to the plankton were chosen to be the most likely source of the additional reverberation in this study [28]. A column strength of –59 dB was calculated for the deepest scattering strength vs. depth profile available at 38 kHz using the data from 25 to 100 m.

Column strengths for the Fram Strait MIZ and those from several other cold-water regions are compared in Fig. 12 [28, 29]. The latitude of all these regions is 3° or farther south than the Fram Strait sites. All the other sites except the Chukchi Sea have peak column strength levels that are higher than those measured in the Fram Strait MIZ at or below 5 kHz. The 38-kHz data from the Chukchi Sea is about the same as the 30-kHz data from MIZ 88 but is 5 dB or more higher than the 40-kHz data. The Davis Strait column strengths, at –55 dB, are 2 to 3 dB higher than Station 2 data at 7.5 and 12 kHz and about the same as the Station 3 data at 16 and 20 kHz. North Baffin Bay data for 5 kHz had the highest value shown, –41 dB. Labrador Sea West data were higher than those in the Fram Strait, with peaks at 1 and 5 kHz and a plateau of –47 dB from 12 to 20 kHz. The Norwegian Sea site shown has a –46 dB peak at 4 kHz and matches the Station 3 data at 16 kHz [29]. This indicates that fish in the Fram Strait in May are smaller and less numerous than those in the other areas shown.

Increased column strengths in the western MIZ 88 data of Station 3 correspond to increased influence of fauna found along the Greenland coast and of the polar water flowing through the Fram Strait into the East Greenland Current. More *A. glacialis* than *B. saida* are found near Greenland

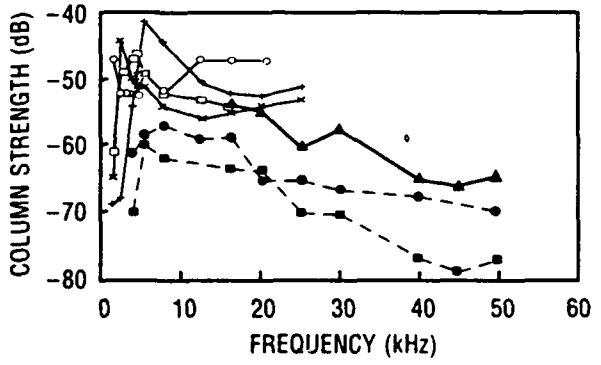

Fig. 12 — Column strength vs. frequency for various cold-water areas in the North Atlantic and Arctic Oceans. ◊ Chukchi Sea MIZ, + North Baffin Bay, × Davis Strait, □ Norwegian Sea (northeast of Iceland), ○ Labrador Sea West, ■ Station 1, ● Station 2, and ▲ Station 3.

and Station 3; however, *B. saida* is the species mentioned in data from the Spitsbergen waters closer to Station 1. This trend distinguishes the stations from each other.

A swimbladder scattering model that relates fish length and depth to resonance scattering was used to link the acoustic measurements with potential biological targets [30]. Since polar cod occur in all parts of the Arctic, have swimbladders, and have been caught in the Fram Strait, they are the most likely fish to be causing volume reverberation at the MIZ 88 experiment sites. *A. glacialis* caught in May in the Chukchi Sea were 8 cm long [25]. Age and length distribution data from the Barents Sea west of 30°E indicates that between April and June of 1986 1-year-old (i.e., 16 to 18 months) *B. saida* were 6 to 9 cm long. Younger fish made up a greater percentage of the catches in the western part of the Barents Sea study [27]. *B. saida* from the Arctic grow more slowly than those in warmer seas. Their larvae drift passively until they are about 1.5 cm long. The ratio of fish length to swimbladder radius for polar cod was estimated to be 25 [31]. An estimate of the length of a fish producing resonant scattering at a given frequency is obtained using the equation

$$L = q\{(z + 10)/10\}^{.5} \; / \; f \, , \tag{2}$$

where L is fish length in centimeters, q is the fish length to swimbladder radius ratio, z is the depth in meters, and f is the frequency in kilohertz. For redfish, 19 would be a reasonable q value [32].

In Fig. 13, frequencies of the highest layer strength for each layer at Station 2 are marked with the length of polar cod whose swimbladders would resonate at those frequencies. These are rough estimates of the fish size for the given frequency and depth range. Layer depths and fish length estimates were similar for all three stations. Above the thermocline, layer strengths for all three stations peaked between 5 and 16 kHz. If this scattering is from polar cod, they are between 1 and 4 cm long. That would indicate mainly 4- to 6-month and, perhaps, at 4 cm, 16- to 18-month-old polar cod that had not grown as fast as those of the same species from farther south. Stations 2 and 3 also have a layer strength peak at 30 kHz above the thermocline. This may be scattering from bubbles in the shells of pteropods with an effective scattering radius about 0.3 mm or from larval fish 6 to 7 mm long. Polar cod that are 5 to 6 cm long could provide scattering layers at the depths and low frequencies of the in-thermocline and below-thermocline layers of Station 1.

Station 2 had a plateau of –64 to –65 dB layer strengths from 5 to 16 kHz in the thermocline, which indicates 1- to 5-cm polar cod. Below the thermocline, Station 2 had a peak at 7.5 kHz, which

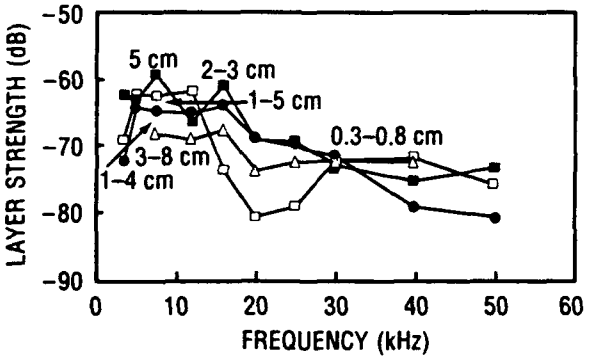

Fig. 13 — Polar cod sizes estimated for peak scattering frequencies at different depth ranges from Station 2. □ Above thermocline, • in thermocline, ■ below thermocline, and Δ deeper than 300 m.

could be from 5-cm polar cod, and another peak at 16 kHz, which gave a fish length estimate between 2 and 3 cm that may be very young polar cod or even shorter redfish. The 300- to 800-m layer peaked from 7.5 to 16 kHz for Station 2. This could be caused by polar cod that are 3 to 8 cm long, or perhaps young Atlantic cod. The 3.5-kHz data at Station 1 has a scattering peak of –70 dB around 900 m that gave the very deep layer a strength of –53 dB. Cod about 21 cm long or deep-water redfish about 16 cm long would produce resonant scattering at that frequency. Adult fish produce scattering at the lower frequencies used in the MIZ 88 experiment. Between 16 and 30 kHz, larval fish and large zooplankton are the dominant scatterers. Saithe spawn at 100- to 200-m depths west of Spitsbergen as late as May [22]. Their larvae would be the right size to contribute to 16 kHz and higher frequency scattering in mid-May [26]. If pelagic wolffish larvae have swimbladders, they could contribute to scattering at these frequencies also. Large groups of tiny organisms, such as copepods, euphausids, or pteropods, produce higher frequency scattering layers.

CONCLUSIONS

Column strengths in the Fram Strait MIZ varied between –50 and –80 dB in the 3.5- to 50-kHz range with a general decrease from low to high frequencies. Levels increased as the ice camp moved toward the Greenland continental shelf. Station 3 had higher levels over all frequencies than the other stations. Although lower windspeeds and a thermocline layer that begins shallower and covers a wider depth range should have made the upper 170 m at Station 3 attractive to fish, a large portion of the total column strength comes from layers below the thermocline. The water of the North Atlantic forms this warmer deep layer. Perhaps the proximity to shallower water off the Greenland continental shelf allowed more zooplankton and *A. glacialis* to inhabit this site.

The variations of layer strength with frequency indicate more than one size of scatterer. Information on midwater fish in this area was obtained mostly from studies of their predators and prey, but *A. glacialis*, *B. saida*, and Atlantic cod have been caught in the Fram Strait. Young polar cod from 2 to 6 cm long are the most likely scatterers in the lower part of the frequency range. Either very young redfish or bubbles trapped in pteropod shells could have been responsible for some of the peak layer strengths at 30 kHz and above. Larval fish less than 1 cm long with tiny swimbladders would be resonant scatterers at these frequencies. Although copepods do not have swimbladders, large colonies of them can contribute to volume reverberation at 50 kHz and above. The strong scattering layers measured in the MIZ 88 experiment are at lower frequencies and are probably caused by small fish that have swimbladders, such as polar cod and redfish.

Column strengths from most other cold-water areas where volume reverberation has been measured are higher than Fram Strait values. Some measurements with levels similar to those at Station 3 were found in the Davis Strait and the Norwegian Sea. Scattering strength levels, which decrease as the frequency changes from 5.0 to 3.5 in the Fram Strait data, indicate that large fish, such as the commercially exploited stocks that produce lower frequency scattering at the other sites shown, are not found in the upper 600 m of the Fram Strait MIZ.

ACKNOWLEDGMENTS

The author thanks Dr. Joe Posey, who was principal investigator, along with Mr. Walt Johnson and Mr. John Selleck of PSI, who were Dr. Posey's primary assistants in performing the volume reverberation experiment. I am especially grateful to Dr. Richard H. Love for his technical assistance

and support of this project. Thanks are also due to the U.S. Coast Guard for providing the USCGC *Northwind* and its crew to make passage into the MIZ possible. This research was supported by the Office of Naval Research. Technical management was provided by the Naval Research Laboratory, Stennis Space Center, under Program Element 0602435N, Project No. RJ35121, Dr. Edward R. Franchi, Program Manager. Dr. Dan J. Ramsdale was the project manager in 1988.

This report includes data presented at the Ocean Reverberation Symposium in May 1992. Some of the same information was also published in an abbreviated form in the Symposium Proceedings by Kluwer Academic Publishers.

REFERENCES

1. Roger W. Meredith, Paul J. Bucca, and Kim McCoy, "Environmental Measurements and Analysis: Arctic Acoustics Experiments in the Marginal Ice Zone," Naval Research Laboratory, Stennis Space Center, MS, NORDA Report 210, August 1989.

2. David G. Ainley and Douglas P. DeMaster, "The Upper Trophic Levels in Polar Marine Ecosystems," in *Polar Oceanography Part B Chemistry, Biology, and Geology*, Walker O. Smith, Jr. ed. (Academic Press, Inc., San Diego, 1990), Ch. 11, pp. 599–629.

3. John B. Garver, Wilbur E. Garrett, and Gilbert M. Grosvenor, "Atlantic/Arctic Ocean Floors," *Supplement to the National Geographic*, **177**(1), 61A (1990).

4. S.L. Smith, "Egg Production and Feeding by Copepods Prior to the Spring Bloom of Phytoplankton in Fram Strait, Greenland Sea," *Mar. Bio.* **106**, 59–69 (1990).

5. Ola M. Johannessen, "MIZEX, the Marginal Ice Zone Experiment," The Nansen Remote Sensing Center, University of Bergen, in *Oceanography and Biology of Arctic Seas*, G. Hempel, ed. (Rapports et Procés-Verbaux des Reunions), Vol. 188 (International Council for Exploration of the Sea, 1989), p. 67.

6. P.A. Moiseev, *The Living Resources of the World Ocean*, Translated from Russian by the Israel Program for Scientific Translations, Jerusalem, 1971, p. 334.

7. Sharon L. Smith, Walker O. Smith, Louis A. Codispoti, and David L. Wilson, "Biological Observations in the Marginal Ice Zone of the East Greenland Sea," *J. Mar. Res.* **43**, 693–717 (1985).

8. Klaus-Günther Barthel, "Feeding of Calanus in the Greenland Sea," in *Oceanography and Biology of Arctic Seas*, G. Hempel, ed. (Rapports et Procés-Verbaux des Reunions), Vol. 188 (International Council for Exploration of the Sea, 1989), pp. 185–205.

9. Sharon L. Smith and Sigrid B. Schnack-Schiel, "Polar Zooplankton," in *Polar Oceanography Part B Chemistry, Biology, and Geology*, Walker O. Smith Jr., ed. (Academic Press, Inc., San Diego, 1990), pp. 527–598.

10. Ole Jørgen Lønne and Bjørn Gulliksen, "Occurrence and Ecological Importance of Sympagic Fauna in the Fram Strait, Svalbard Area and Western Barents Sea," in *Oceanography and*

Biology of Arctic Seas, G. Hempel, ed. (Rapports et Procés-Verbaux des Reunions), Vol. 188 (International Council for Exploration of the Sea, 1989), p. 170.

11. Sibbjørn Mehl, "The Northeast Arctic Cod Stock's Consumption of Commercially Exploited Prey Species in 1984–1986," in *Oceanography and Biology of Arctic Seas*, G. Hempel, ed. (Rapports et Procés-Verbaux des Reunions), Vol. 188 (International Council for Exploration of the Sea, 1989), pp. 185–205.

12. C. Richard Robins and G. Carleton Ray, *A Field Guide to Atlantic Coast Fishes of North America* (Houghton-Mifflin Company, Boston, MA, 1986), p. 92.

13. A.P. Andriashev, "Fishes of the Northern Seas of the USSR," Akademiya Nauk SSSR Zoological Institute (Keys to the fauna of the USSR 53), 1954 Translated from the Russian by Israel Program for Scientific Translations, 1964.

14. C.F. von Dorrien, D. Piepenburg, and M.K. Schmid, "On the Abundance of Arctic Cod Arctogadus Glacialis in Northeast Water," *Polar Record* pp. 362–364 (1991).

15. P.J.P. Whitehead, M.-L. Bauchot, J.-C. Hureau, J. Nielsen, and E. Tortonese, *Fishes of Northeastern Atlantic and the Mediterranean* (United Nations Educational, Scientific, and Cultural Organization, Paris, France, 1984, 1986, 1986), Vols. I, II, and III.

16. P.J.P. Whitehead, M.-L. Bauchot, J.-C. Hureau, J. Nielsen, and E. Tortonese, *Fishes of Northeastern Atlantic and the Mediterranean* (United Nations Educational, Scientific, and Cultural Organization, Paris, France, 1986), Vol. III, pp. 1115–1116.

17. P.J.P. Whitehead, M.-L. Bauchot, J.-C. Hureau, J. Nielsen, and E. Tortonese, *Fishes of Northeastern Atlantic and the Mediterranean* (United Nations Educational, Scientific, and Cultural Organization, Paris, France, 1986), Vol. III, pp. 1225–1227.

18. P.J.P. Whitehead, M.-L. Bauchot, J.-C. Hureau, J. Nielsen, and E. Tortonese, *Fishes of Northeastern Atlantic and the Mediterranean* (United Nations Educational, Scientific, and Cultural Organization, Paris, France, 1986), Vol. III, pp. 1282–1283.

19. George Brown Goode and Tarleton H. Bean, *Oceanic Ichthyology: A Treatise on the Deep-Sea and Pelagic Fishes of the World* (Smithsonian Institution United States National Museum, 1895).

20. P.J.P. Whitehead, M.-L. Bauchot, J.-C. Hureau, J. Nielsen, and E. Tortonese, *Fishes of Northeastern Atlantic and the Mediterranean* (United Nations Educational, Scientific, and Cultural Organization, Paris, France, 1986), Vol. II, pp. 680–693.

21. P.J.P. Whitehead, M.-L. Bauchot, J.-C. Hureau, J. Nielsen, and E. Tortonese, *Fishes of Northeastern Atlantic and the Mediterranean* (United Nations Educational, Scientific, and Cultural Organization, Paris, France, 1984), Vol. I, pp. 143–144.

22. P.J.P. Whitehead, M.-L. Bauchot, J.-C. Hureau, J. Nielsen, and E. Tortonese, *Fishes of Northeastern Atlantic and the Mediterranean* (United Nations Educational, Scientific, and Cultural Organization, Paris, France, 1986), Vol. II, pp. 682–691.

23. Richard Ellis, "Marine Mammals of the World," *Whalewatcher Journal of the American Cetacean Society* (1982).

24. R.J. Urick, *Principles of Underwater Sound* (McGraw-Hill Book Company, New York, New York, 1975) pp. 214–216.

25. W.J. Hansen and M.J. Dunbar, "Biological Causes of Scattering in the Arctic Ocean," Proceedings of an International Symposium on Biological Sound Scattering in the Ocean, G. Brooke Farquhar, ed., Maury Center for Ocean Science, Department of the Navy, Washington, D.C. 1970, pp. 508–526.

26. G. Brooke Farquhar, "Biological Scattering in the Barents Sea," unpublished report Naval Oceanographic and Atmospheric Research Laboratory, NOARL Liaison Office, Arlington, VA, 1990.

27. Terje Monstad and Harald Gjøsæter, "Observations on Polar Cod (*Boreogadus saida*) in the Barents Sea 1973 to 1986," International Council for the Exploration of the Sea, C.M. 1987/G:13.

28. G.R. Garrison, E.A. Pence, H.R. Feldman, and S.R. Shah, "Studies in the Marginal Ice Zone of the Chukchi Sea: Analysis of 1972 Data," APL-UW 7311, March 1974.

29. R.P. Chapman, O.Z. Bluy, R.H. Adlington, and A.E. Robinson, "Deep Scattering Layer Spectra in the Atlantic and Pacific Oceans and Adjacent Seas," *J. Acoust. Soc. Am.* **56**, 1722–1734 (1974).

30. R.H. Love, "Resonant Acoustic Scattering by Swimbladder-Bearing Fish," *J. Acoust. Soc. Am.*, **64**, 571–580 (1978).

31. W.B. Scott and M.G. Scott, "Atlantic Fishes of Canada," *Can. Bull. Fish. Aquat. Sci.*, **219**, 260–270 (1988).

32. R. H. Love, Naval Research Laboratory, Stennis Space Center, MS, personal communication (1992).